

Abstract

Concurrent observations of geomagnetic variations by means of a fluxgate magnetometer and an induction magnetometer were carried out at Syowa (L=6.3) and Mizuho Stations(L=7.7) in Antarctica from August 29 to September 29, 1973. Spectral and polarization characteristics of the substorm-associated Pi2 pulsations are investigated in detail using the data obtained at Syowa and Mizuho as well as those at Mawson(L=9.1), Sanae(L=4), Hermanus (L=1.8) in the southern hemisphere and Reykjavik(L=6.3) in the northern hemisphere. The Pi2 pulsations are observed simultaneously with the onset of a substorm expansion phase over the wide area from the auroral region to the low latitudes with a similar predominant period showing a primary amplitude maximum at the auroral oval and a secondary one near the plasmapause. Pi2 period is closely related to the location of the auroral breakup region in the following way that it becomes shorter(longer) when the auroral breakup occurs at lower(higher) latitude. The Pi2 data from the conjugate pair of stations, Syowa and Reykjavik, show that the H-components oscillate in phase, whereas the D-components oscillate out of phase suggesting that Pi2 waves observed in the auroral region are characterized as odd mode standing oscillations. The characteristics of Pi2 polarization change drastically across the center of the auroral electrojet. The sense of polarization reverses from a left-hand polarization on the lower latitude side of the auroral electrojet to a right-hand one on the higher latitude side before ~21h MLT at which Pi2 maximum occurrence is observed and vice versa after ~21h MLT. Such polarization reversals result from large phase shifts(~180°) of the horizontal(north-south) components across the center of the auroral electrojet. If Pi2 waves propagate westward before the time of Pi2 maximum occurrence and eastward thereafter, the observed polarization reversals can be interpreted by the resonance theory of the coupled hydromagnetic waves. Considering these observational results, the torsional hydromagnetic oscillation of the field lines localized at the auroral oval is the most plausible model for a main cause of Pi2 pulsations.

1. Introduction

It is well known that during magnetospheric substorms, various types of ultra-low frequency electromagnetic waves or so-called geomagnetic Pi pulsations are observed. Most of these waves are thought to be generated in the magnetosphere and propagate in the magnetospheric medium as hydro-magnetic waves. This phenomenon is called as a magnetic pulsation substorm, and is one of the important manifestations of the magnetospheric substorm (AKASOFU, 1968, 1977). In association with the onset of a magnetospheric substorm expansion phase, Pi2 pulsations are observed over the wide area from the auroral region to low latitudes on the ground, as well as in the magnetosphere (SAITO, 1969; SAITO and SAKURAI, 1970; FUKUNISHI and HIRASAWA, 1970; PERKINS *et al.*, 1972; OLSON and ROSTOKER, 1975; LANZEROTTI *et al.*, 1976; SAITO *et al.*, 1976a; PYTTE *et al.*, 1976). The purpose of this paper is to clarify wave characteristics of Pi2 pulsations based on the data simultaneously observed in the auroral region, plasmopause and low latitudes and to examine their generation mechanism.

Since the first report by ANGENHEISTER(1912), Pi2 pulsations have been investigated by many research workers. It was once called under a name of night- or Pt-type pulsations, and then classified as Pi2 pulsations at the Berkeley Meeting of IAGA(1963). Pi2 pulsations are essentially nightside phenomena showing its maximum occurrence around local midnight(KATO *et al.*, 1956; YANAGIHARA, 1960; HIRASAWA and NAGATA, 1966).

Careful inspections of Pi2 pulsations show that their occurrence maximum is found slightly before the local midnight(*e.g.*, 22h–23h LT in Fig. 6 of YANAGIHARA, 1960). SAITO and MATSUSHITA (1968) showed that the local time of maximum occurrence of Pi2 pulsations varied from year to year between 22h and 01h LT, and they suggested that it has a systematic recurrence tendency caused by the solar rotation. According to the results by SMITH (1973), Pi2 maximum occurrence is observed near 2330 LT during intervals of low magnetic activity, while it is observed near 2030 LT during intervals of high magnetic activity. The variation of the maximum occurrence time

may be related to the solar wind streaming angle as shown in Fig. 3 of SMITH (1973). The observed variation of the solar wind direction with magnetic activity may cause such a change in the magnetotail axis, thereby the shift of the Pi2 source region.

Pi2 pulsations are observed simultaneously over the wide area from the auroral region to the low-latitudes as damped-type magnetic oscillations with a predominant period in the range of 40 ~ 150 sec. The Pi2 period varies greatly with geomagnetic activity. It becomes shorter(longer) when the geomagnetic activity increases(decreases) (TROITSKAYA, 1967; SAITO and MATSUSHITA, 1968). On the other hand, the latitudes of both the auroral oval (AKASOFU and CHAPMAN, 1963; STRINGER and BELON, 1967; FELDSTEIN and STARKOV, 1968) and the plasmopause(CARPENTER and STONE, 1967; BINSACK, 1967; RYCROFT and THOMAS, 1970) shift toward lower(higher) latitude in a higher(lower) magnetic activity. Thus, a close relation between the Pi2 period and the extent of the magnetospheric cavity will be strongly suggested from those observational results.

The latitude dependence of the Pi2 amplitude shows a primary maximum in the auroral region(SAITO, 1969; OLSON and ROSTOKER, 1975) and a secondary one near the plasmopause(RASPOPOV *et al.*, 1972; SAITO *et al.*, 1976). ROSTOKER (1967), SAITO and SAKURAI(1970), RASPOPOV *et al.*(1972) and SAITO *et al.*(1976) suggested that Pi2 pulsations are caused by torsional eigen oscillations of the local field lines anchored on the auroral oval. On the other hand, FUKUNISHI and HIRASAWA(1970) found that the Pi2 pulsations observed at low latitudes have more sinusoidal waveforms than those of the Pi2 observed in the auroral region. FUKUNISHI and HIRASAWA(1970) and SUTCLIFFE (1975b) proposed that low-latitude Pi2 pulsations are due to transient surface waves on the plasmopause excited by high latitude hydromagnetic disturbances associated with the substorm. Recently, OLSON and ROSTOKER(1977) suggested clear contributions of the ionospheric currents to the Pi2 generation based on the data showing a close relation between the auroral electrojet and the Pi2 intensity. They concluded that Pi2 pulsations observed in the auroral region are not generated by simple magnetohydrodynamic oscillations of magnetic field lines. OLSON and ROSTOKER(1977) and WILHELM *et al.* (1977) proposed that changes in the magnetospheric and ionospheric current systems are a main cause of Pi2 pulsations in the auroral region.

Wave characteristics of Pi2 pulsation will be best examined by studying their polarization behavior. However, many contradicting observation have been reported on polarization characteristics of Pi2 waves. The results obtained at low-latitude stations(KATO *et al.*, 1956; SUTCLIFFE, 1975a) indicate that Pi2 pulsations are right-hand polarized in the local pre-midnight hours and left-hand polarized in the post-midnight hours. On the other hand,

CHRISTOFFEL and LINFORD(1966) and ROSTOKER(1967) showed that Pi2 waves observed in the sub-auroral region are predominantly left-hand polarized, regardless of local time. According to the investigations by BJÖRSSON(1971) and FUKUNISHI(1975), the sense of Pi2 polarization reverses across the plasma-pause from a left-hand polarization on the lower-latitude side to a right-hand polarization on the higher-latitude side. SAKURAI(1970) showed statistically that the sense of Pi2 polarization at College (64.7° in geomagnetic latitude) changes from a predominantly left-hand polarization in the local pre-midnight hours to a predominantly right-hand polarization in the post-midnight hours, whereas Pi2 events at Point Barrow(68.5° in geomagnetic latitude) are predominantly right-hand polarized, regardless of local time. However, polarization characteristics of Pi2's in the auroral region have not yet been clarified. Moreover, a relation between locations of auroras in breakup events and Pi2 polarization characteristics is still uncertain. Conjugate relationships of Pi2 pulsations in the auroral region have also not clarified.

In order to study wave characteristics and generation mechanism of Pi2 pulsations which show drastic variations in the course of the substorm, it is necessary to make concurrent observations at the ground-based stations situated along the same geomagnetic meridian. Such observations were carried out by means of fluxgate magnetometers and induction magnetometers at Mizuho(L=7.7) and Syowa Stations(L=6.3) by the 14th wintering party of the Japanese Antarctic Research Expedition during the period from August 29 to September 29, 1973(KUWASHIMA, 1974a and b). In the present paper, the general characteristics of Pi2 waves will be discussed on the basis of the data obtained at Mizuho and Syowa, as well as those from Mawson(L=9.1), Sanae(L=4) and Hermanus (L=1.8) in the southern hemisphere and Reykjavik (L=6.3) in the northern hemisphere. The five stations mentioned above are located in a geomagnetic longitude range from 43.6° (Sanae) to 93.2° (Mawson). The locations of these stations, the facilities for the observations of geophysical phenomena at Mizuho and Syowa Stations and the data analysis methods will be described in Chapter 2. Relations between auroral motions and the associated magnetic variations are discussed and the method for determining the location of the center of current will be examined in Chapter 3. In Chapter 4, spectral features of Pi2 pulsations are studied and then relations between Pi2 period and the locations at which auroral breakup occurred will be described. The spatial distributions of Pi2 polarization around the auroral electrojet are studied in Chapter 5. Chapter 6 describes wave phase relations of Pi2's at the conjugate station, (Syowa and Reykjavik). Some examinations are applied to the observed results and a possible generation mechanism of the Pi2 pulsations will be discussed in Chapter 7.

2. Experiment and Data Analysis

2.1. Observing instruments at Mizuho and Syowa Stations

During the period from August 29, to September 29, 1973, continuous observations of geomagnetic variations by means of fluxgate magnetometers and induction magnetometers were carried out at Syowa and Mizuho Stations in Antarctica. Syowa Station ($69^{\circ}00'S$, $39^{\circ}35'E$ in geographic coordinates) is located at latitude -66.7° and longitude 72.4° in corrected geomagnetic coordinates. Mizuho Station ($70^{\circ}42'S$, $44^{\circ}17'E$ in geographic coordinates) located at ~ 260 km from Syowa towards the Geomagnetic South Pole is an inland station which was established in 1970 as an observatory for glaciology and meteorology. Mizuho (-68.7° and 72.9° in corrected geomagnetic coordinates) is located on almost the same geomagnetic meridian as that of Syowa. Geomagnetic local time (MLT) of these two stations is approximately same as universal time (UT), while geographic local time (LT) is about 3 hours earlier than UT.

Block diagrams of the observing facilities which were installed at both Mizuho and Syowa are illustrated in Fig. 1. Main part of the induction magnetometers of the two stations consists of sensors, d.c. amplifier, a PWM analog data recorder and a monitoring pen oscillograph. The S/N ratio in the final stage is generally larger than 40 dB. The frequency response curves of H-component at the both stations are illustrated in Fig. 2.

The main part of the fluxgate magnetometer installed at Mizuho is essentially equivalent to that at Syowa. It consists of three orthogonal sensors, carrier oscillators, phase comparators, d.c. amplifiers and pen recorders. Back-ground magnetic field was cancelled by means of NKS magnets at Mizuho, and by the electrical method using the Helmholtz coil at Syowa.

In addition to the induction and fluxgate magnetometers, the following instruments were installed at Syowa for the upper atmosphere research.

(a) Geomagnetism

3-component high-sensitive rapid-run magnetometer (0.5 nT/mm and 300mm/hour).

Fig. 1. Block diagrams of the observing systems which were installed at both Mizuho and Syowa Stations(upper part) and the analyzing system(lower part). Spectral analyzer is a SD 360 Digital Signal Processor designed by the Spectral Dynamics Corporation (USA). H 10-II is a minicomputer (HITAC 10-II) designed by the Hitachi Manufactory (Japan).

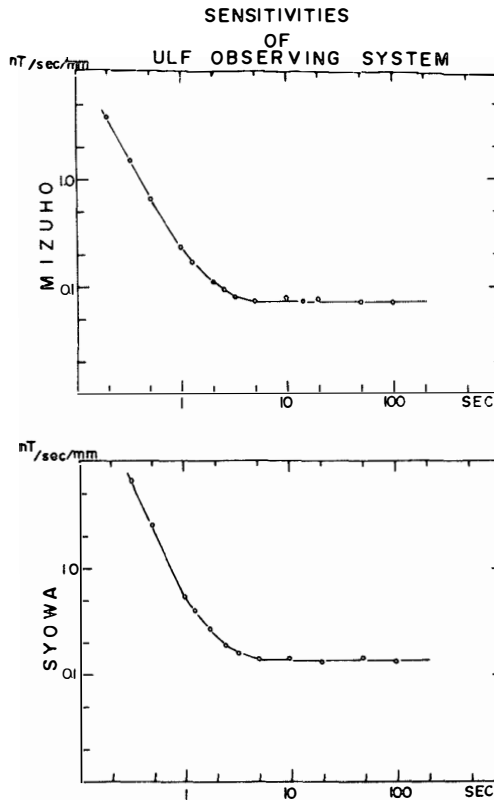
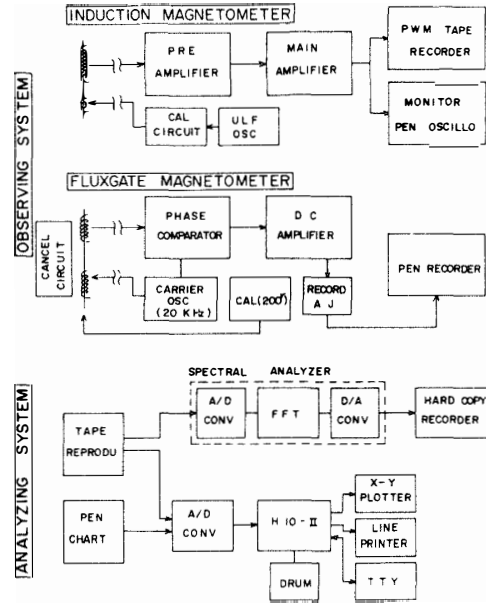


Fig. 2. Sensitivities of the induction magnetometer on chart records at Mizuho and Syowa Stations.

- (b) Aurora
 - (i) 35mm all-sky camera with a fish-eye lens (6 frames/min).
 - (ii) Meridian-scanning photometers for measurement of electron auroras (4278Å, 5577Å, 6300Å) and proton aurora (4861Å).
 - (iii) Zenith photometers for measurement of 4278Å emissions (5° and 30° fields of view).
- (c) Ionosphere
 - (i) Ionosonde for bottomside sounding operated every 15 minutes.
 - (ii) Riometers ($f=10, 20, 30, 50$ and 70 MHz).
- (d) VLF emissions
 - (i) Narrow-band field intensity recorders ($f=0.3, 0.5, 0.7, 1.0, 1.4$ and 2.0 kHz for chorus emissions, and $4, 8, 16, 32, 64$ and 128 kHz for auroral hiss).
 - (ii) Magnetic tape recorder for continuous recording with a tape speed of 4.75 cm/sec (frequency range of 0.2 to 4.0 kHz).

2.2. Locations of the stations

The pulsation data from Mawson, Sanae, Hermanus and Memambetsu are used in the present investigation. Mawson is located about 2° poleward side of Mizuho. Sanae (South Africa National Antarctic Expedition) is located

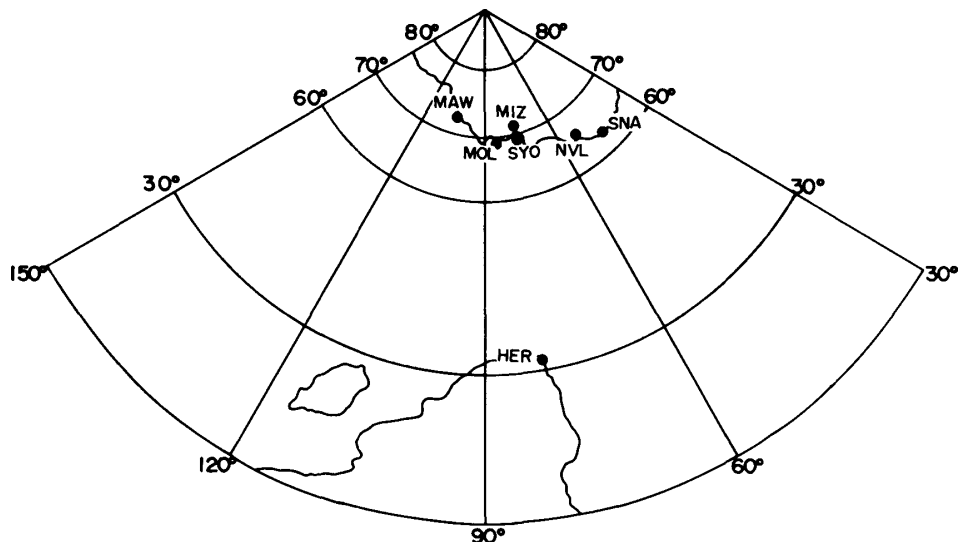


Fig. 3. Location of the southern hemisphere magnetometer stations in geomagnetic coordinates. Reykjavik in the northern hemisphere is the conjugate station of Syowa. MAW.: Mawson, MIZ.: Mizuho, SYO.: Syowa, MOL.: Molodezhnaya, NVL.: Novolazarevskaya, SNA.: Sanae, HER.: Hermanus.

on the lower latitude side of Syowa and in the neighborhood of the plasmapause. It is worthy of notice that the low latitude station, Hermanus, is located along almost the same geomagnetic meridian as those of Syowa and Mizuho.

The rapid-run magnetograms from Reykjavik which is a geomagnetically conjugate station of Syowa are used for studying conjugacy of Pi2 pulsations. In addition to those data, the normal-run magnetograms from Mawson, Molodezhnaya, Novolazarevskaya and Sanae are also used. The geomagnetic locations of these stations are shown in Fig. 3 as well as in Table 1, respectively.

Table 1. Geomagnetic locations.

Station	Corrected latitude	Geo-magnetic longitude	Induction magnetogram	Normal-run magnetogram	Rapid-run magnetogram	L value
Mawson	-70.6°	93.2°	○	○		9.1
Mizuho Station	-68.7°	72.9°	○	○	○	7.7
Syowa Station	-66.7°	72.4°	○	○	○	6.3
Novolazarevskaya	-62.7°	51.8°		○		4.8
Sanae	-60.0°	43.6°	○	○		4.0
Hermanus	-41.0°	79.7°	○	○		1.8
Reykjavik	66.6°	71.2°		○	○	6.3
Memambetsu	34.0°	208.4°	○	○		1.6

2.3. Data analysis

A block diagram of the analysis system of magnetic pulsations is illustrated in Fig. 1. As is shown in the figure, it consists of two parts, one is an spectral analyzer for data recorded on analog magnetic tape and the other is a minicomputer(HITAC 10-II) for digital data.

The spectral analyzer is SD 360 Digital Signal Processor designed by the Spectral Dynamics Corporation in USA and executes spectral analysis in a Fast Fourier Transform Method(FFT). The minicomputer is HITAC 10-II(HIO-II) designed by the Hitachi Manufactory in Japan. The digital power spectra are calculated by means of the minicomputer using an improved new method which is suitable for the analysis of irregular magnetic pulsations. This method has great advantages comparing with other conventional methods (BURG, 1972; SMYLIE *et al.*, 1973; CURRIE, 1974; SUTCLIFFE, 1975a; ULRYCH and BISHOP, 1975).

In this section, the reliability of this method is examined in comparison with conventional methods (the Blackman-Tukey and FFT methods). In the Blackman-Tukey method, the power spectrum is given by the Fourier transform of the autocorrelation function (BLACKMAN and TUKEY, 1958). Assuming the following time sequence which consists of the data sampled at equispaced intervals Δt ,

$$\{X(i)\} \quad i = 1, \dots, N$$

the autocorrelation function is given by

$$\Phi(n) = \frac{1}{N} \sum_{i=1}^{N-n} X(i)X(i+n) \quad n=0, 1, 2, \dots, M \quad (1)$$

where n is the lag number with a maximum lag value M . Then the power spectral density function (PSD) is derived from the following relation,

$$P(f) = 2 \cdot \Delta t \left(\Phi(0) + 2 \sum_{n=1}^{M-1} \Phi(n) \cos \frac{\pi \cdot k \cdot n}{M} + \Phi(M) \cos \frac{\pi \cdot k}{M} \right)$$

$$f = \frac{k}{2M \cdot \Delta t} \quad k=0, 1, 2, \dots, M. \quad (2)$$

On the other hand, in the FFT method the PSD is defined as the absolute value squared of the Fourier coefficient of the original time sequence.

The Fourier coefficient is given by,

$$F(n) = \sum_{i=0}^{N-1} X(i) \cdot \exp \left\{ -j \frac{2\pi i n}{N} \right\} \quad n=0, \dots, N-1 \quad (3)$$

and PSD is derived from the following equation,

$$P(f) = \frac{2 \cdot \Delta t}{N} |F(n)|^2 \quad n=0, \dots, N-1. \quad (4)$$

However, since the length of the time sequence is finite, it is necessary to make an unrealistic assumption about the data outside its available range. Thus, in performing the spectral analysis, a probable data window should be applied to the autocorrelation functions before obtaining the PSD by the Blackman-Tukey method, whereas a data window should be applied to the time sequence before obtaining the Fourier coefficients by the FFT method. The problems which arise in the above analysis techniques are leakage, frequency shifts, statistical variability and limited resolution. In those two conventional spectral methods, the bandwidth of the spectrum must be broad in order to obtain statistically reliable spectral estimates, and alternatively if the bandwidth is so narrow as to give an sufficient resolution, the estimated spectrum becomes unreliable (SUTCLIFFE, 1975a). Band widths are $B_e = 1/M \cdot \Delta t$ for the Blackman-Tukey method, while $B_e = m/N \cdot \Delta t$ for the FFT method, where m is the number of contiguous estimates averaged. This problem becomes especially noticeable when time series of short length are analyzed.

The maximum entropy method (MEM) has been devised at first by BURG

(1967) for estimating the spectra with increased resolution. This method is considered to be the most useful for short length of data such as Pi pulsations. In the MEM, PSD is calculated from the following relation,

$$P(f) = \frac{P_M}{fn} \left[1 + \sum_{n=1}^M a_n \cdot \exp\{-i2\pi fn\Delta t\} \right]^{-2} . \quad (5)$$

$$fn = \frac{1}{2 \cdot \Delta t} \quad : \text{Nyquist frequency}$$

$\{a_n\}$, $n=1, \dots, M$: the prediction-error filter

P_M : the mean output power of the filter

It is obvious from eq.(5) that the bandwidth constraint which exists in the conventional methods are eliminated, because $P(f)$ can be calculated for arbitrary values of frequency. Two methods are proposed for the estimation of $\{a_n\}$ and P_M . The method devised by BURG (1967) uses a recursive algorithm, and the other devised by AKAIKE(ULRYCH and BISHOP, 1975) is known as an auto-regressive spectral estimate. In the Akaike's method, the length of the prediction error filter M is adopted when it minimizes the $(FPE)_M$ which is defined as follows,

$$(FPE)_M = \frac{N+M+1}{N-M-1} P_M . \quad (6)$$

Reliabilities of those methods are compared using artificially generated

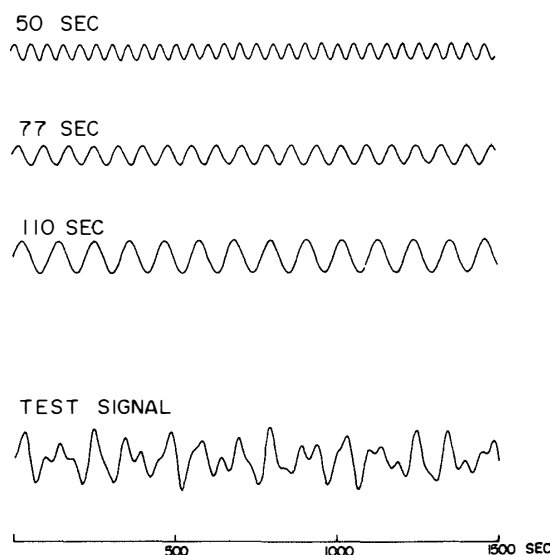


Fig. 4. Waveforms of the monochromatic and compounded waves which are used for the comparison of the efficiencies of the four different spectral analysis methods(Blackman-Tukey, Fast Fourier Transform, Maximum Entropy Method (AKAIKE) and Maximum Entropy Method (BURG)).

time sequence, which is similar to those of the irregular magnetic pulsations. The waveform of this time sequence as well as that of each monochromatic wave component is illustrated in Fig. 4. The time sequence was generated from the equation

$$TS = 10.0 \sin(2\pi \cdot \Delta t / 110) + 6.0 \sin(2\pi \cdot \Delta t / 77) + 5.0 \sin(2\pi \cdot \Delta t / 50), \quad \Delta t = 5 \text{ sec.}$$

The power spectra of this wave were calculated by means of Blackman-Tukey, FFT, MEM(AKAIKE) and MEM(BURG), and are illustrated in Figs. 5a, b, c and d, respectively. It is obvious from the figures that MEM is much superior to the Blackman-Tukey and FFT methods with high resolution of the spectral

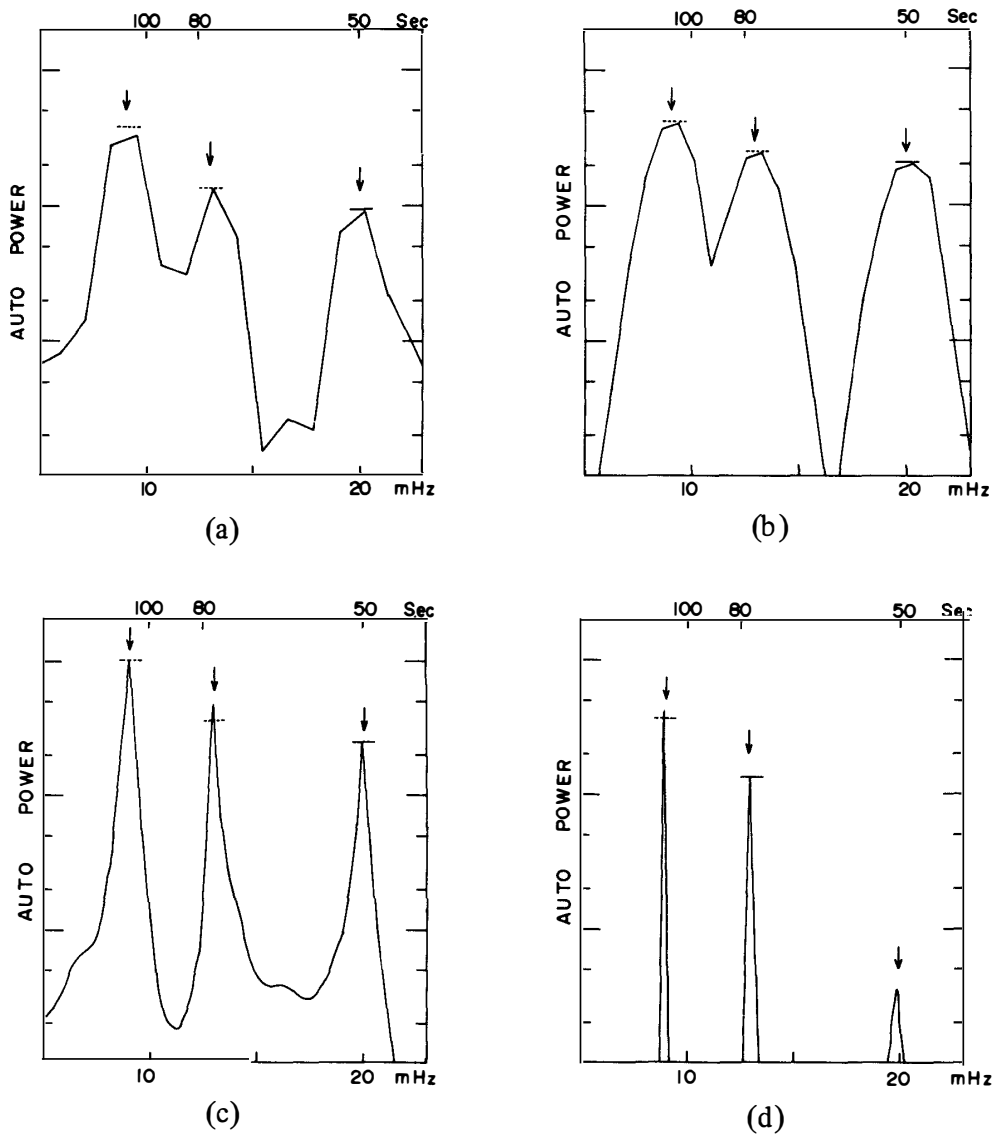


Fig. 5. Auto-power spectra calculated by means of Blackman-Tukey(a), Fast Fourier Transform(b), Maximum Entropy Method(AKAIKE)(c) and Maximum Entropy Method(BURG)(d).

peak. The spectra in Fig. 5 were calculated in the long interval (1280 sec). In a case of short length of time sequence (*e.g.* 300 sec), MEM can still detect each wave component contained in the test signals, whereas the conventional two methods cannot detect sufficiently each wave component. From this reason, MEM seems to be very useful for transient phenomena such as Pi pulsations.

As shown in Figs. 5c and d, the spectra calculated by the Burg method show sharper spectral peaks than those by the Akaike method. However, spectral powers estimated by the former method are not always equal to those expected from the original wave amplitudes, which are marked on the figure by the bar. This tendency was pointed out also by SUTCLIFFE (1975a). On the other hand, spectral powers estimated by the latter method seem to be approximately equal to those expected from the original wave amplitude. In the present work, the Akaike method is applied to the spectral analysis of Pi pulsations because of the above mentioned reasons.

3. Estimation of Latitude of Auroral Breakup Event

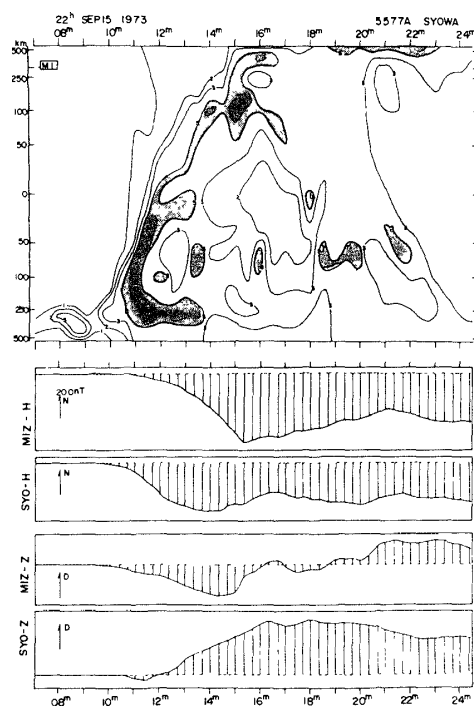
It is well known that Pi pulsations are closely associated with magnetospheric substorm(auroral substorm). Therefore, it is necessary to study the relationship between occurrence regions of auroral breakup events and Pi pulsations. In this chapter, a method for an estimation of the auroral breakup region by means of the ground-based magnetic data in the auroral region is discussed.

3.1. Relationship between auroral motion and magnetic variation

Dynamical behavior of aurora is examined by means of records of all sky camera or geomagnetic meridian scanning photometer data. Fig.6 (upper) shows an example of the space-time diagram of auroral luminosity, which was made from the scanning photometer record at Syowa. An outline of the geomagnetic meridian scanning photometer and a practical method for making the space-time diagrams of auroral luminosity is given in the paper of HIRASAWA and NAGATA(1972) or FUKUNISHI and TOHMATSU(1973). In the ordinate of the auroral diagram in Fig. 6, 0 km corresponds to the zenith of Syowa. Assuming the auroral average height to be 100 km, the poleward horizon of Syowa is about 600 km south (-72° in corrected geomagnetic latitude). Mizuho is located at ~ 260 km poleward from Syowa.

AKASOFU(1965, 1968) has pointed out that the first indication of the auroral substorm is a sudden brightening of the quiet arc lying in the midnight sector of the auroral oval. Within a few minutes after the brightening, the rayed arcs suddenly become active and show rapid poleward motions; this phenomenon is a so-called "auroral breakup". The auroral behavior in Fig. 6 is generally consistent with a view given by AKASOFU. As is seen in the auroral diagram, the auroral brightening began at about 2208 UT on September 15, 1973 at a location of ~ 250 km equatorward from Syowa. At about 2210 UT, the aurora started to move poleward with a large increase in luminosity and passed over the zenith of Syowa at about two minutes after the onset of the poleward expansion (2212 UT) and arrived around

Fig. 6. Space-time diagram of electron aurora (5577 \AA) at Syowa and simultaneously observed magnetic variations in H- and Z-components at Mizuho and Syowa Stations on September 15, 1973. Numerals of the isointensity contours of electron aurora are given in unit of 500 rayleighs



the zenith of Mizuho at about 2216 UT with the speed of ~ 1.5 km/sec on the average. Accompanied with this auroral breakup, the negative changes of the magnetic H-component were seen at both Syowa and Mizuho. The time, when the H-component reached a minimum, almost coincides with the time when the aurora arrived at the zenith of each station. When the aurora was located at the zenith of the observing stations (2212 UT at Syowa and 2216 UT at Mizuho), the Z-component intensities returned nearly to the pre-substorm level. When the aurora was located at the equatorward (poleward) of the station, the Z-component showed an upward (downward) change.

Two successive poleward travelings of the aurora started at about 2143:30 and 2151:00 UT on September 22, 1973 as shown in Fig. 7. In association with auroral motions, drastic variations in the Z-component magnetic fields are also found in this event.

Fig. 8 shows that small auroral breakup event occurred successively three times. A close relationship between auroral motions and magnetic variations is seen even in these small substorm events.

In the examples in Figs. 6–8, the brightening and the poleward movement of aurora were accompanied by the negative change in the H-component. On the other hand, the direction of the Z-component is opposite between

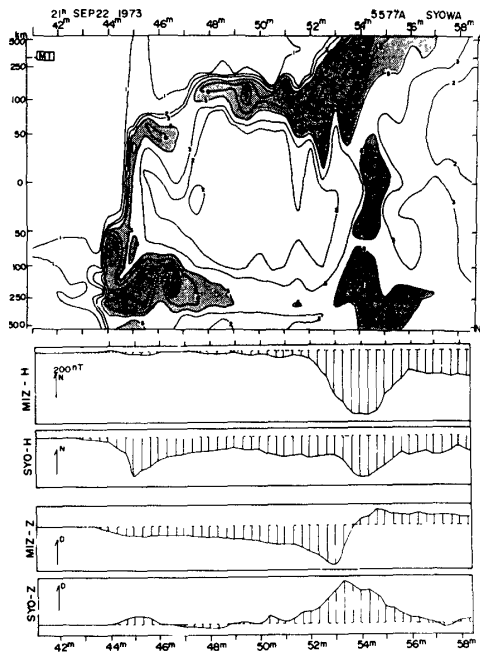


Fig. 7. Space-time diagram of electron aurora at Syowa(5577 A) and simultaneously observed magnetic variations at Mizuho and Syowa Stations on September 22, 1973.

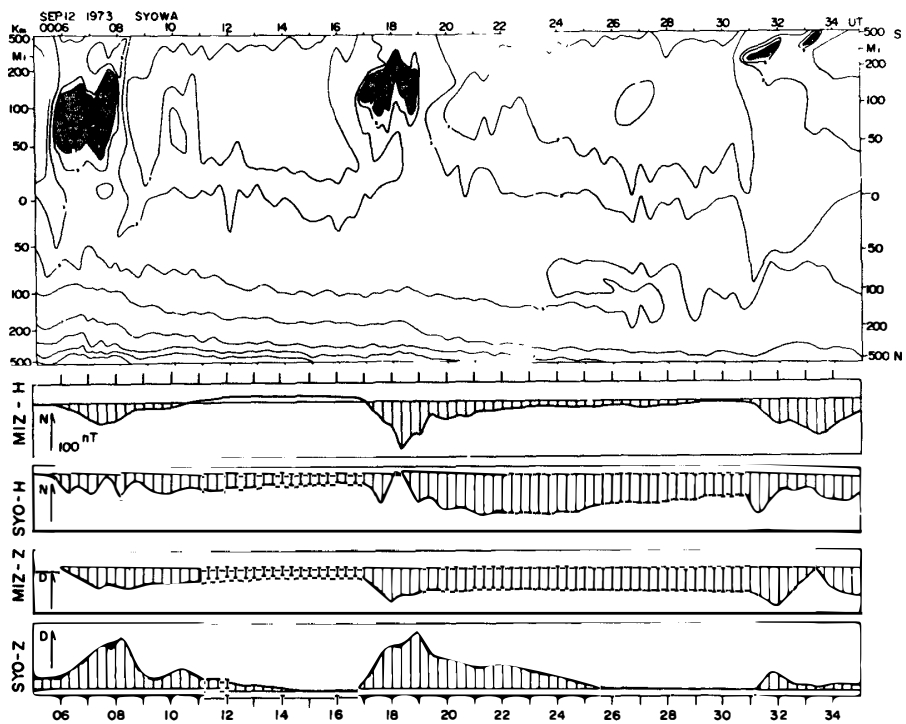


Fig. 8. Space-time diagram of electron aurora at Syowa(5577 A) and simultaneously observed magnetic variations at Mizuho and Syowa Stations on September 12, 1973.

the poleward and equatorward regions of the brightest aurora. The Z-component returned to the pre-storm level when the active aurora reaches near the zenith of the observing station. Those relations between auroral motions and magnetic variations may be interpreted on the assumption that a westward auroral electrojet is strongly localized in the latitudinal direction like a line current with a large length in the longitudinal direction. Under this condition, the magnitude of the H-component will be much larger than that of the D-component. The magnitude of the H- and Z-components will reach a minimum and zero, respectively, when the center of westward auroral electrojet is located at the zenith of the observing station. The direction of the Z-component derivation is opposite in the poleward(upward) and the equatorward(downward) of the electrojet in the southern hemisphere and vice versa in the northern hemisphere.

Fig. 9 shows a series of latitude profiles of the H-, D- and Z-components

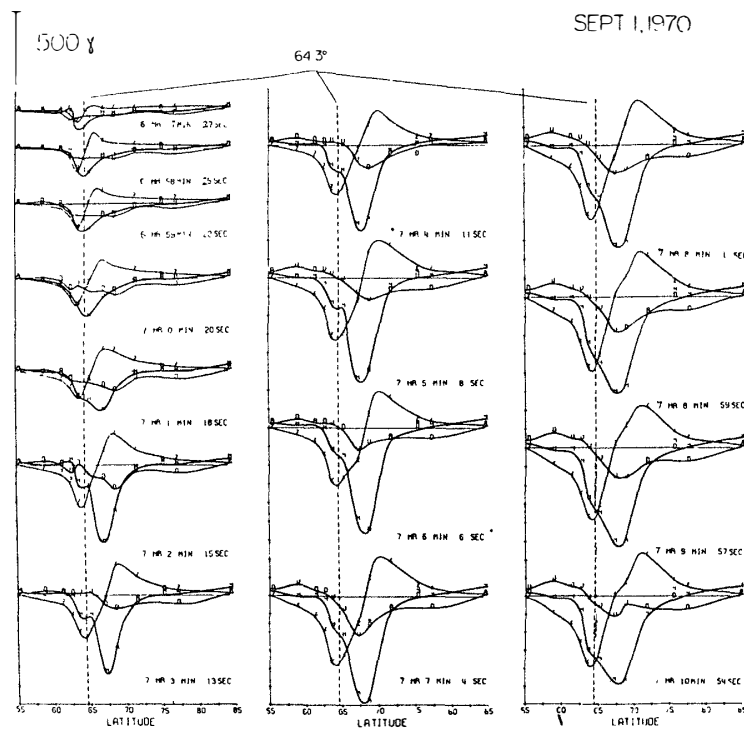


Fig. 9. Series of latitude profiles (~ 1 -min intervals) showing the development and poleward expansion of the current system during the substorm expansive phase. As shown in the figure, the magnitude of the H-component reaches minimum when the current system comes to the zenith of the observing station ($\Delta Z=0$). Magnitude of the D-component variation is smaller than that of the H-component. The dashed vertical line represents the latitude at which the current system began to develop (After KISABETH and ROSTOKER, 1974).

during the substorm expansion phase in the midnight hours, which is obtained on the basis of the data from the University of Alberta meridian chain of magnetometers (KISABETH and ROSTOKER, 1974). The behaviors of magnetic variations in the H- and Z-components in Fig.9 are similar to those in Figs. 6–8. The magnitude of the H-component reaches minimum at the region under the auroral electrojet, where the variation of the Z-component is very small ($\Delta Z=0$). The sense of the Z-component changes from upward in the equatorward side of the auroral electrojet to downward in the poleward side of the auroral electrojet (in the northern hemisphere). The range of the D-component variation is considerably smaller than that of the H-component one in the course of the substorm expansive phase. The result suggests that the direction of the auroral electrojet is nearly westward.

The magnetic behaviors shown in Figs. 6–9 give an evidence that the line current model for the auroral electrojet can represent fairly well the features of the magnetic perturbation associated with the substorm events in the auroral region.

3.2. Estimation of latitude of auroral breakup region from magnetic data

On the assumption of the line current model for the auroral electrojet, the latitude at which the auroral breakup event occurred was estimated by comparing between magnetic variations at Syowa and Mizuho Stations. During the period from August 29 to September 29, 1973, eleven auroral breakup events were identified by both the auroral space-time diagrams at Syowa and the magnetic data at Syowa and Mizuho. Fig.10 shows the relation between the latitudes of auroral breakup events estimated from the auroral space-time diagrams (ordinate) and those of the centers of auroral electrojet

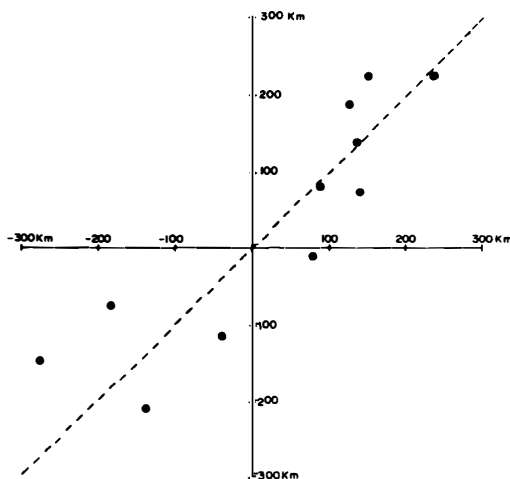


Fig. 10. Relations between the location of auroral breakup estimated from the auroral diagram (ordinate) and that from the magnetic variations (abscissa). The origin corresponds to the zenith of Syowa. The positive (negative) values on both the ordinate and abscissa mean that the auroral breakup occurred on the poleward side (equatorward side) of Syowa. If two values derived from the two different methods were identical, they would be located on the dashed line ($y=x$).

currents estimated from the Biot-Savart's law under the line current model (abscissa). The origin in Fig.10 corresponds to the zenith of Syowa. A poleward direction is measured upward in the ordinate and to the right in the abscissa. If the latitudes estimated by the two methods were identical, they would be located on the dashed line ($y=x$). In Fig.10, eleven points analyzed here are located in the neighborhood of the dashed line. This fact shows that the line current model is useful for estimation of the auroral breakup region in the first order approximation.

During the period from August 29 to September 29, 1973, ninety magnetic substorm events were observed at Syowa and at Mizuho. For the eleven events, the latitudes of auroral breakup regions were estimated by both the auroral diagrams and magnetic data from Syowa, Mizuho and Mawson. For the twenty-eight events, the latitudes of auroral breakup regions were estimated by means of both the all-sky photographs and the magnetic data. For the thirty-nine events, the latitudes of auroral breakup regions were estimated by only the magnetic data. For the remaining twelve events, their auroral breakup positions cannot be estimated.

4. Spectra of the Pi Pulsations

In this chapter, spectral features of Pi pulsations observed during the substorm expansion phase are examined on the basis of the data obtained at Mizuho(L=7.7), Syowa(L=6.3), Sanae(L=4.0), Hermanus(L=1.8) and Mawson(L=9.1) in the southern hemisphere and at Reykjavik(L=6.3) in the northern hemisphere.

At middle- and low-latitude stations, damped type pulsations (Pi2) are observed in coincidence with the onset of the substorm expansion phase. On the other hand, waveforms of Pi pulsations observed at auroral stations are generally irregular, probably due to an effect of random fluctuations of ionospheric currents caused by auroral ionization. As is pointed out by KUWASHIMA(1975), Pi pulsations observed at auroral stations in the beginning of substorms consist of Pi burst (irregular waveforms and localized) and Pi2 (regular waveforms and observed over wide area). Therefore, it is difficult to find out from original waveform records in the auroral region the Pi2 component corresponding to that at middle- and low-latitudes. In order to exclude the above-mentioned difficulties, a numerical band-pass filtering technique is used here. The filter is a Gaussian-type filter, which is designed to take out the Pi2 component from original records for a period range from 40 to 150 sec with -3 dB high-cut and low-cut characteristics. Pi2 pulsations analyzed in the present paper is damped type pulsations simultaneously observed with the onset of substorm expansion phase over a wide area from the auroral region to the low-latitudes with a predominant period ranging from 40 to 150 sec. Spectral features of the Pi2 are investigated by means of digital power spectra. Details of the method of data treatments have been already given in Chapter 2.

4.1. Examples of the Pi spectra

Fig. 11a shows an example of H and Z variations in a substorm event. The start of the magnetic substorm expansion phase is identified as a sudden decrease of the H-component of Syowa at about 2020 UT. Judging from

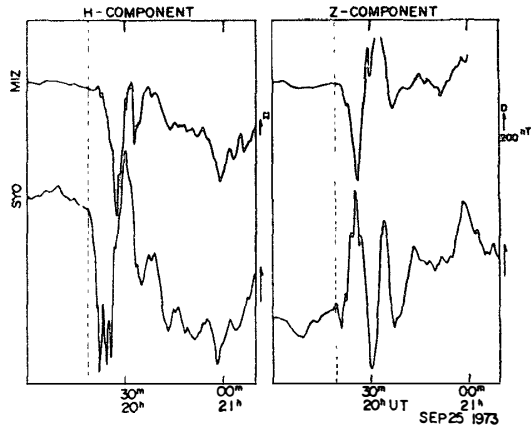


Fig. 11a. Magnetic variations of the H- and Z-components simultaneously observed at Mizuho and Syowa Stations on September 25, 1973. The substorm expansion started at about 2020 UT.

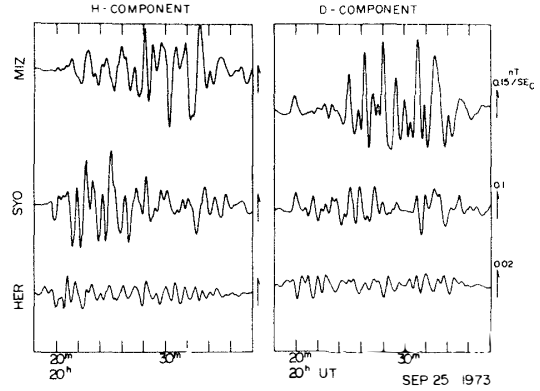


Fig. 11b. Band-pass filtered wave trains of the Pi pulsations observed over the wide area from the auroral region to the low latitude. The substorm expansion started at about 2020 UT on September 25, 1973 (cf. Fig. 11a).

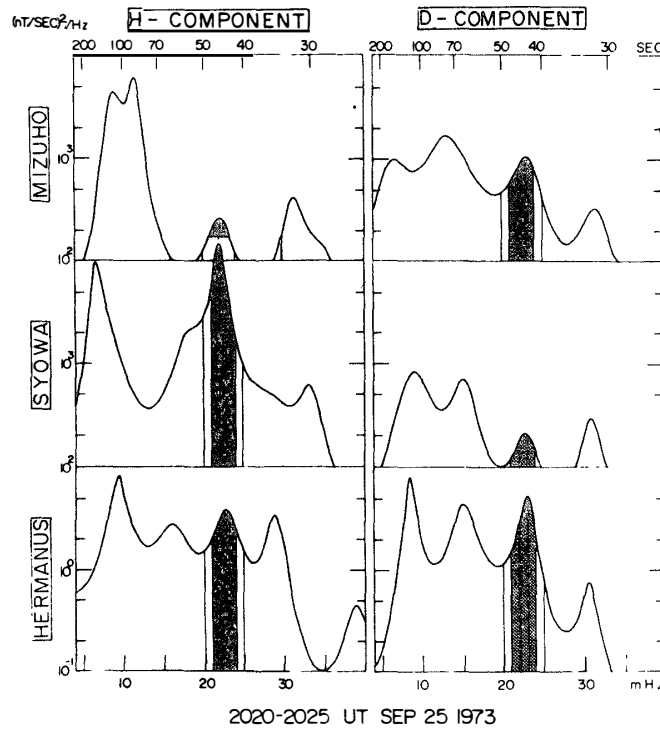


Fig. 11c. Power spectra of the Pi pulsations calculated in the interval of 2020–2025 UT on September 25, 1973, overlapping the data of Fig. 11b.

the Z-component variation, this auroral breakup occurred on a little equatorward of Syowa. In coincidence with the onset of this substorm, Pi pulsations appeared over the wide area from the auroral region to the low-latitudes. The band-pass filtered wave trains of this Pi event in the course of this substorm expansion are illustrated in Fig.11b. In the figure, a sudden intensification of the Pi pulsation was observed almost coincident with the onset of a sharp negative change in the H-component at 2020 UT. The power spectra of the wave trains in Fig.11b were computed in the interval from 2020 to 2025 UT and are shown in Fig.11c. All spectra have several dominant peaks suggesting somewhat irregular waveforms. However, a common peak around 22.5 mHz(44 sec) can be found in these spectra. Such component will be defined as the Pi2 hereafter.

The characteristics of the Pi spectra above-mentioned are also seen in the August 31, 1973 event in which auroral breakup occurred between Mizuho and Syowa at about 0006 UT. The band-pass filtered waveforms

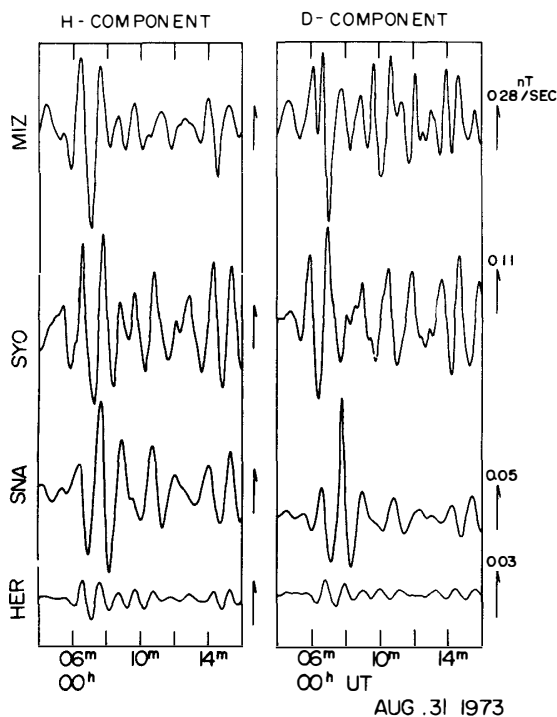


Fig. 12a. Band-pass filtered wave trains of the Pi pulsations observed over the wide area from the auroral region to the low latitude. The substorm expansion started at about 0006 UT on August 31, 1973.

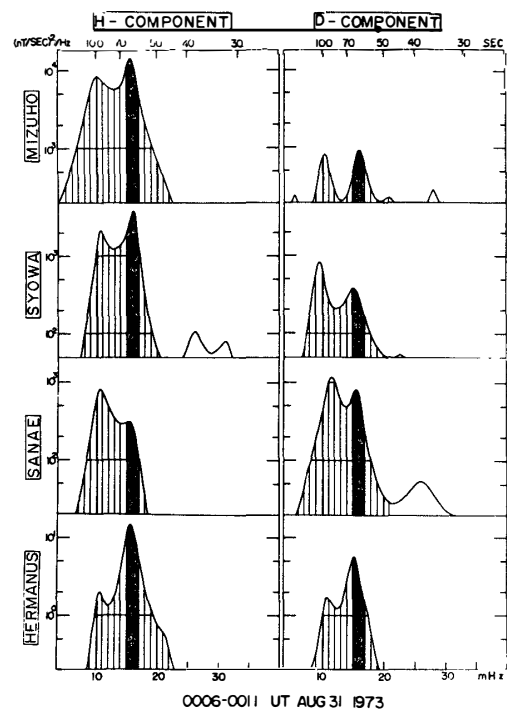


Fig. 12b. Power spectra of the Pi pulsations calculated in the interval of 0006-0011 UT on August 31, 1973, overlapping the data of Fig. 12a.

at the early stage of this substorm are illustrated in Fig. 12a. The Pi events occurred simultaneously at all four stations at about 0006 UT, coincident with the onset of the sharp negative change of the H-component at Syowa. The spectra of this event, computed in the interval of 0006–0011 UT, are shown in Fig. 12b. In the figure, all spectra have a common spectral peak around 15.8 mHz(63 sec) and this 63 sec component is considered as the Pi2.

Pi spectra, especially in the auroral region, have several dominant peaks probably due to irregularities in the ionospheric current. For the purpose of reducing an effect of the ionospheric current, spectral features of Pi pulsations associated with small substorms are investigated. Magnetic variations during small magnetic substorm on September 14, 1973 are illustrated in Fig. 13a. The decrease in the H-component began at about 2340 UT at both Mizuho and Syowa and reached a minimum of -96 nT at Mizuho and -62 nT at Syowa, respectively. A small change of the AE index at about 2340 UT may indicate the onset of the substorm. The band-pass filtered wave trains are illustrated in Fig. 13b. Power spectra computed in the interval of 2340–2345 UT are shown in Fig. 13c. At Mizuho, which is located in the auroral region, the spectrum has a relatively dominant spectral component around 16 mHz(62 sec) in the H-component, suggesting that the effect of the auroral current was weak during this small substorm event. In this event, Pi intensity at Syowa was very small compared with that at Mizuho. The

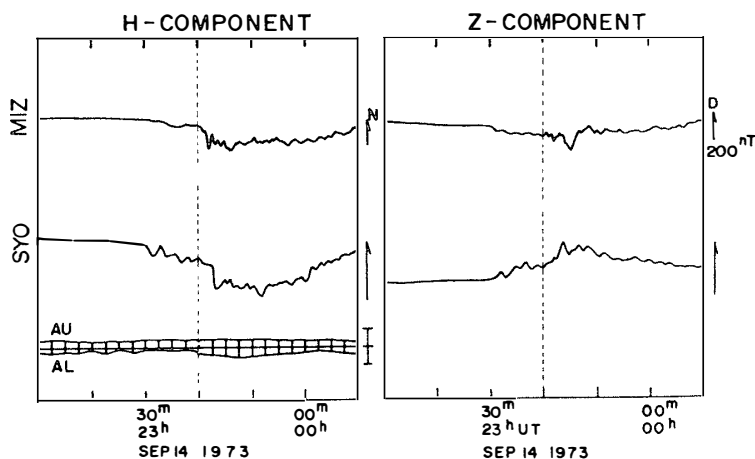


Fig. 13a. Magnetic variations of the H- and Z-components simultaneously observed at Mizuho and Syowa Stations on September 14, 1973, AU and AL indices made at NOAA. The substorm expansion started at about 2340 UT.

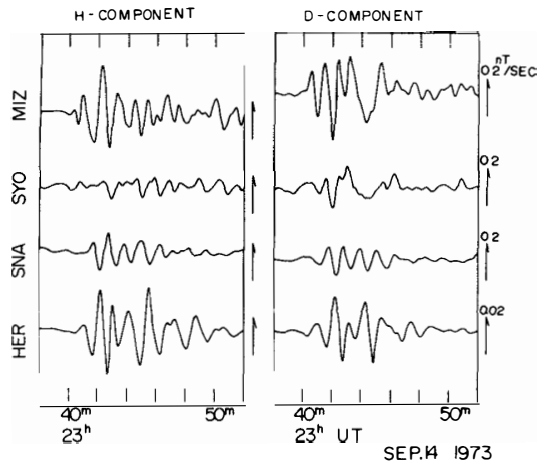


Fig. 13b. Band-pass filtered wave trains of the Pi pulsations observed over the wide area from the auroral region to the low latitude. The substorm started at about 2340 UT on September 14, 1973(cf. Fig. 13a).

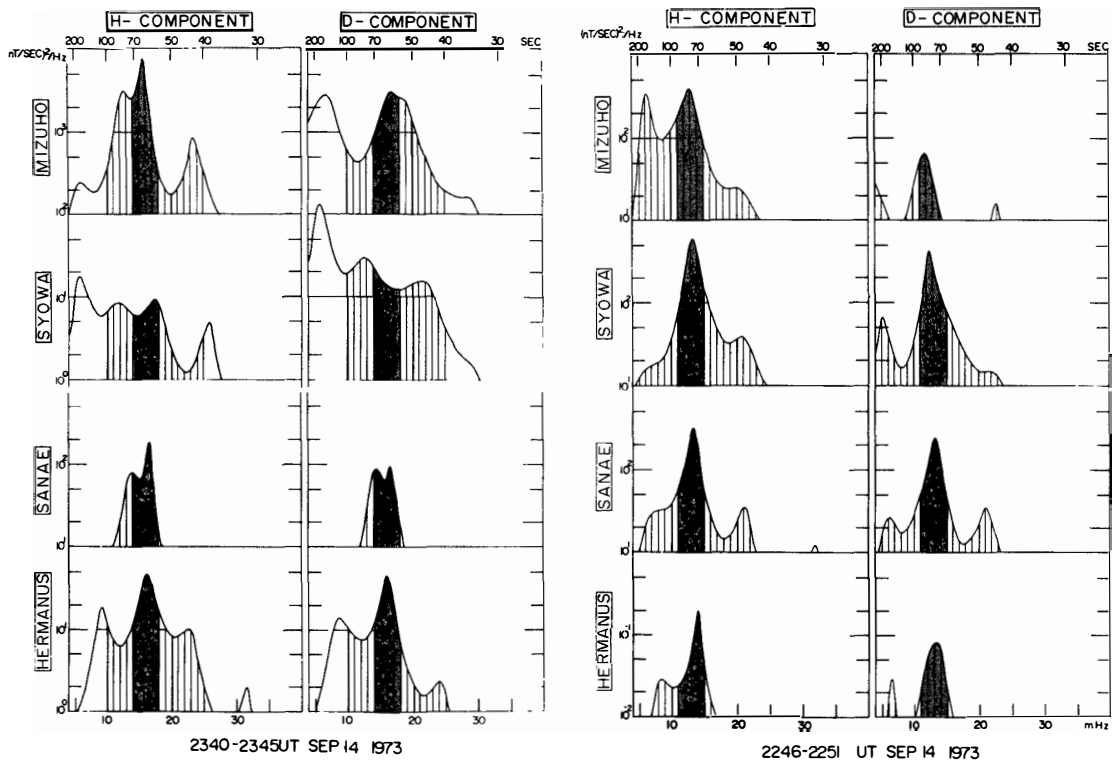


Fig. 13c. Power spectra of the Pi pulsations calculated in the interval of 2340–2345 UT on September 14, 1973, overlapping the data of Fig. 13b.

Fig. 13d. Power spectra of the Pi pulsations calculated in the interval of 2246–2251 UT on September 14, 1973.

62 sec component which is dominant at Mizuho is also observed in the H- and D-component at Sanae and Hermanus. The horizontal power spectral density of the Pi2 is about 8.4×10^4 (nT/sec)²/Hz at Mizuho and 2.3×10^1 (nT/sec)²/Hz at Hermanus. These values are comparable to those associated with the large substorm in company with intense auroral electrojet (*cf.* Figs. 11c and 12b). Another example of Pi spectra observed during a small substorm are shown in Fig. 13d. Dominant spectral peak around 13 mHz (~75 sec) is seen at all four stations. These two events shows that Pi2 can be observed over the wide area even when the associated magnetic substorm is very small.

4.2. Relationship between Pi2 period and latitude of auroral breakup region: Case study

As to the Pi2 period, many research workers (TROITSKAYA, 1967; ROSTOKER, 1967; SAITO and SAKURAI, 1970) indicated that when K_p increases (decreases) the dominant period of Pi2 pulsations becomes shorter (longer). SAITO and SAKURAI (1976) suggested that Pi2 period decreases as the latitude of the auroral oval shifts towards the equator.

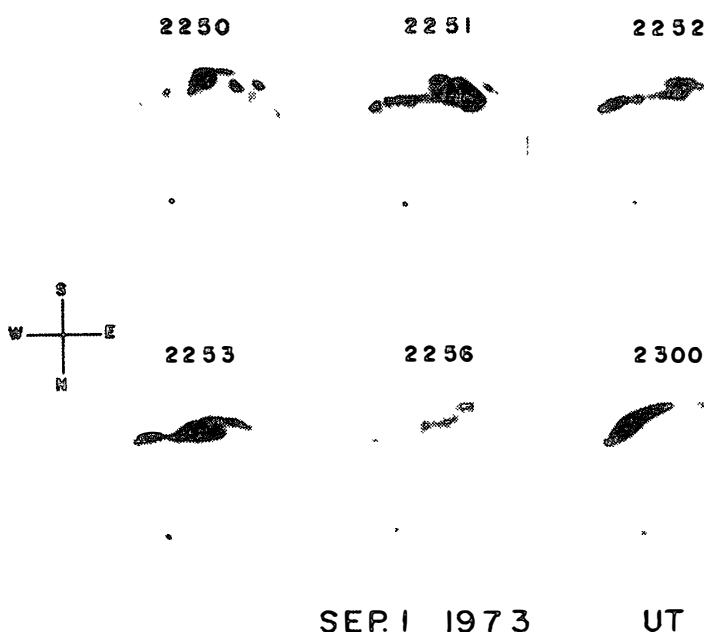


Fig. 14a. All-sky camera photographs at Syowa in one minute interval. Aurora became active at about 2250 UT on September 1, 1973 on the pole-side horizon of Syowa.

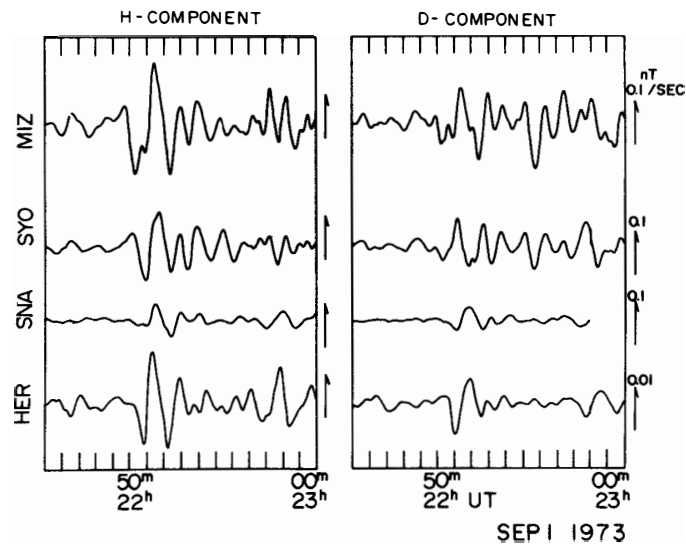


Fig. 14b. Band-pass filtered wave trains of the Pi pulsations observed over the wide area from the auroral region to the low latitude. The sub-storm expansion started at about 2250 UT on September 1, 1973(cf. Fig. 14a).

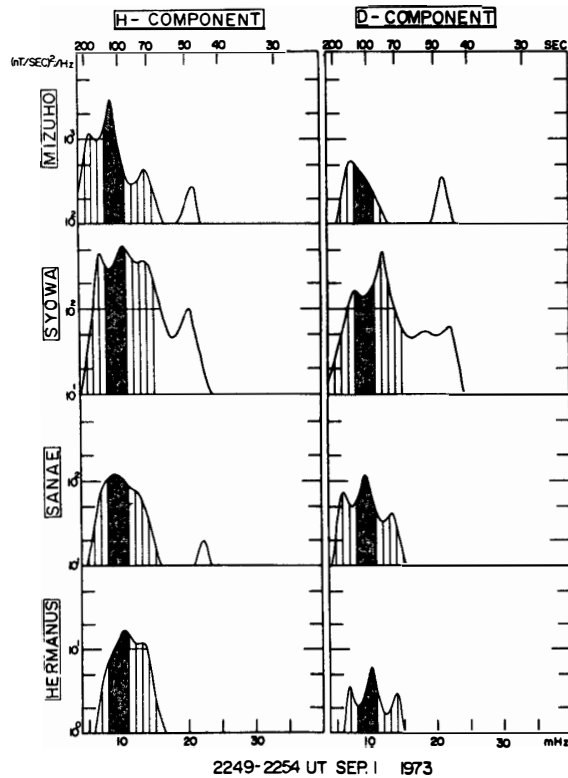


Fig. 14c. Power spectra of the Pi pulsations calculated in the interval of 2249–2254 UT on September 1, 1973, overlapping the data of Fig. 14b.

As is shown in Fig. 14a, aurora becomes active on the poleward of Syowa (-66.7°) and Mizuho (-68.7°) around 2250 UT on September 1, 1973. The estimated geomagnetic latitude of the occurrence region of this auroral breakup event is about -69.5° . In association with this breakup, Pi pulsations were observed over the wide area from the auroral region to the low latitude (Fig. 14b). The power spectra computed in the interval of 2249–2254 UT are shown in Fig. 14c. As is shown in the figure, spectral features are very complicated in this event. However, dominant spectral peaks are found around 100 sec ($10 \text{ mHz} \pm 2 \text{ mHz}$) at each station.

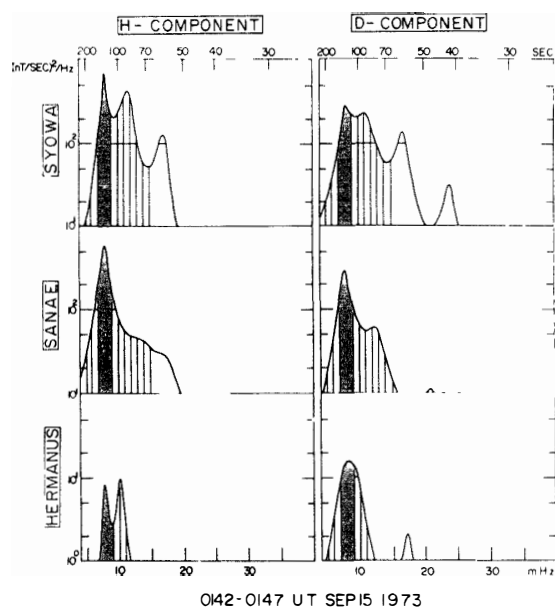


Fig. 15. Power spectra of the Pi pulsations calculated in the interval of 0142–0147 UT on September 15, 1973. Substorm expansion started at about 0142 UT on the poleward side of Mizuho and Syowa Stations

In the September 15, 1973 event the auroral breakup occurred on the poleward side at Mizuho at $\sim -71^\circ$ in geomagnetic latitude. The power spectra of the Pi pulsations observed in this substorm expansion are computed in the interval of 0142–0147 UT and are shown in Fig. 15. As is shown in the figure, each spectrum shows a dominant peak around 7.7 mHz (130 sec). This 130 sec component is considered as the Pi2. The period of the Pi2 associated with the substorm whose auroral breakup occurred at a higher latitude than Syowa and Mizuho is somewhat longer compared with those presented in the previous section.

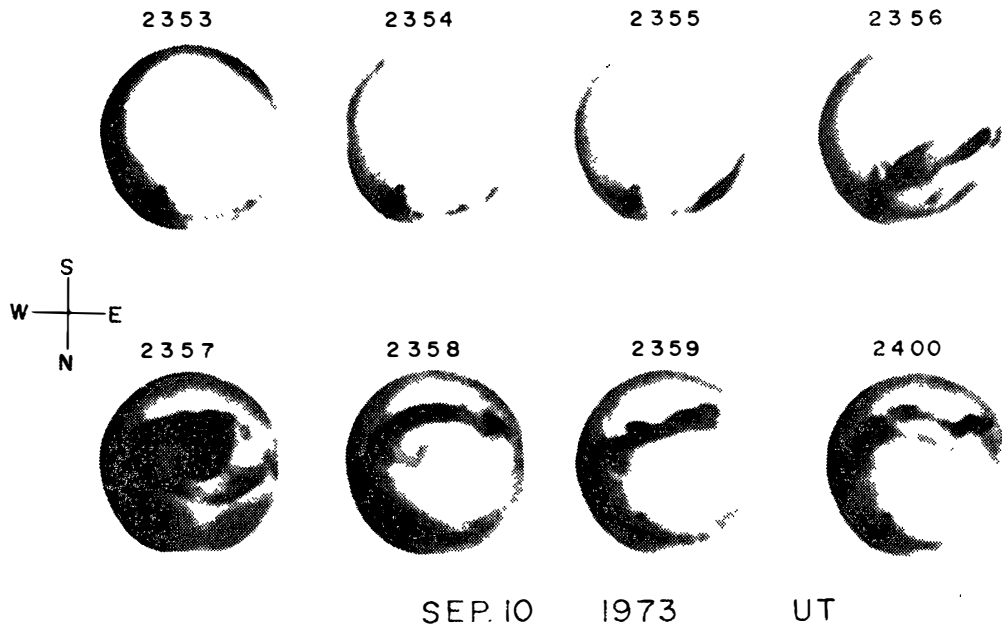


Fig. 16a. All-sky camera photographs at Syowa in one minute interval. Auroral poleward expansion started at about 2354 UT on September 10, 1973 on the equatorward side of Syowa.

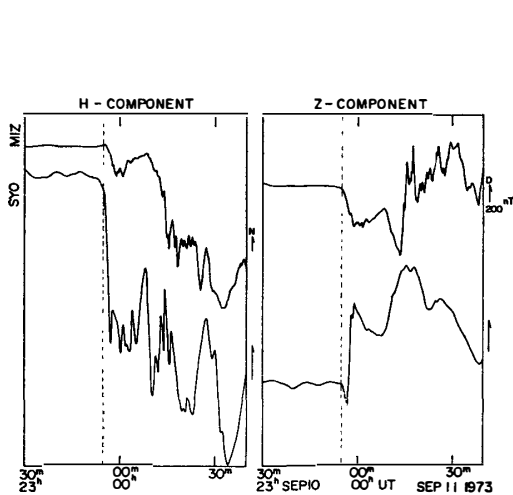


Fig. 16b. Magnetic variations of the H- and Z-components simultaneously observed at Mizuho and Syowa Stations on September 10, 1973. The substorm expansion started at about 2354 UT.

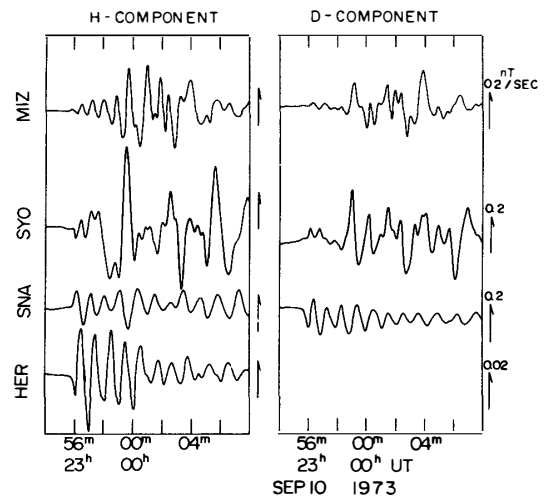


Fig. 16c. Band-pass filtered wave trains of the Pi pulsations observed over the wide area from the auroral region to the low latitude. The substorm expansion started at about 2354 UT on September 10, 1973 (cf. Figs. 15a and b).

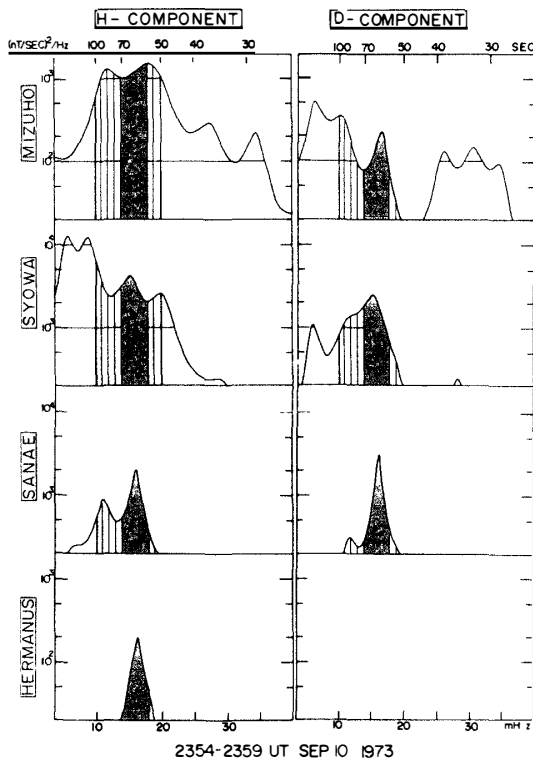


Fig 16d. Power spectra of the Pi pulsations calculated in the interval of 2354–2359 UT on September 10, 1973, overlapping the data of Fig. 15c.

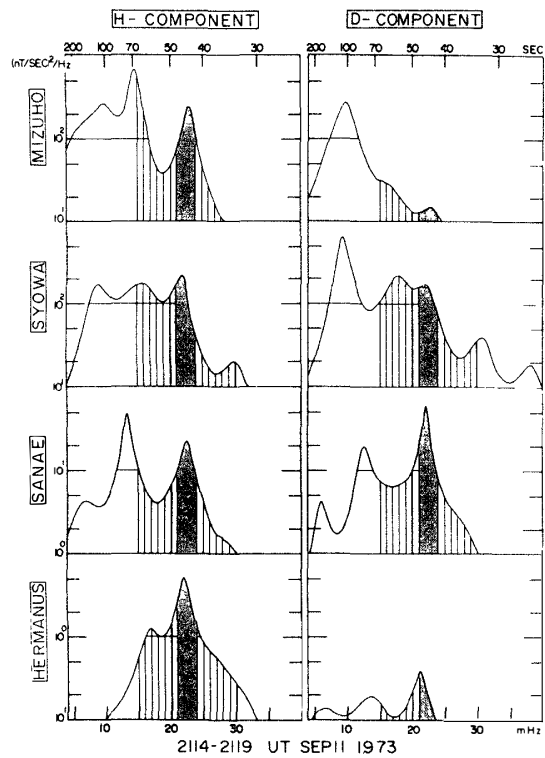


Fig. 16e. Power spectra of the Pi pulsations calculated in the interval of 2114–2119 UT on September 11, 1973.

Figs. 16a–e give another example of Pi2. Judging from the all-sky photographs (Fig. 16a) and magnetograms (Fig. 16b), it is found that the auroral breakup occurred on the equator side of Syowa at about 2354 UT. The estimated geomagnetic latitude of the occurrence region of this auroral breakup event is about 64.5° . The band-pass filtered wave trains of Pi pulsations are illustrated in Fig. 16c. Simultaneously with the start of the H-component sharp decrease and the rapid poleward expansion of the aurora, Pi pulsations began at all four stations. The power spectra computed in the interval of 2354–2359 UT are shown in Fig. 16d. The spectra at Mizuho and Syowa have several peaks indicating somewhat irregular waveforms. However, dominant spectral components around 60 sec ($16 \text{ mHz} \pm 1.5 \text{ mHz}$) is seen at all stations. The period of this Pi2 component is much shorter than the period of those previously presented. Another example of Pi spectra whose associated auroral breakup event occurred at the lower latitude ($\sim 65.5^\circ$) of Syowa are shown in Fig. 16e. In the figure, predominant spectral component around 22 mHz ($\sim 45 \text{ sec}$) is clearly seen at four stations.

4.3. Spectral features of the Pi2 associated with the multiple onset substorm

It has been noticed that several Pi2's are apt to take place successively. Owing to this nature, the Pi2 was once called "pulsation train" or Pt. Because of a close association between Pi2 and magnetospheric substorm (SAITO *et al.*, 1976; SAKURAI and SAITO, 1976), successive Pi2 occurrences probably correspond to multiple onsets of substorms. SAITO *et al.* (1976) have analyzed Pi2 events statistically for the year 1958, on the basis of the IGY Report of the Onagawa Magnetic Observatory (KATO *et al.*, 1961) and concluded that approximately 27 % of substorms have more than one individual Pi2. FUKUNISHI and HIRASAWA (1970) showed on the basis of the data obtained at Memambetsu from January to December, 1966 that the number of the Pi2 wave trains ranges from 1 to 6, most frequently at 2. They also showed that the time interval between two successive Pi2 waves is about 10–20 minutes. Recently, PYTTE *et al.* (1976) investigated the data from two satellites (OGO 5 and Vela 4A) and they found the successive formation of an X-type neutral line (field line reconnection) at an interval of 10–15 minutes. Considering these observational results, the time interval of 10 minutes or so seems to be physically meaningful for the multiple onset substorm. The criterion for the multiple onset substorm used in this paper is successive auroral breakups or successive H-component decreases within the interval of 10 minutes or so.

As shown in Fig. 17a, two small auroral breakups occurred successively within 10 minutes interval. The auroral diagram and the magnetograms in Fig. 17a show that the location of auroral breakup event shifted from low

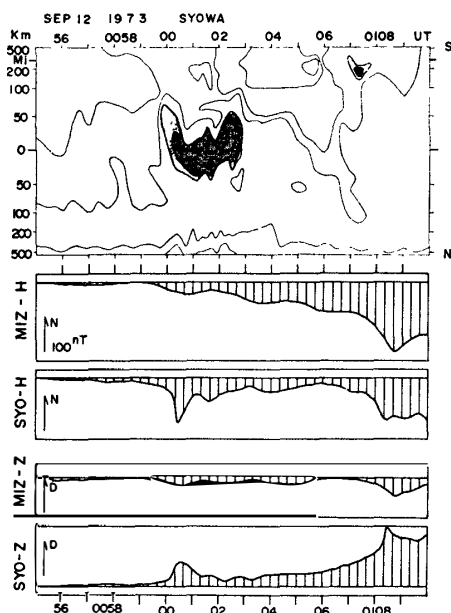


Fig. 17a. Space-time diagram of electron aurora at Syowa (5577 Å) and simultaneously observed magnetic variations of the H- and Z-components at Mizuho and Syowa Stations on September 12, 1973. Two successive substorm expansions started at about 0100 and 0107 UT, respectively.

Wave Characteristics of Magnetic Pi2 Pulsations

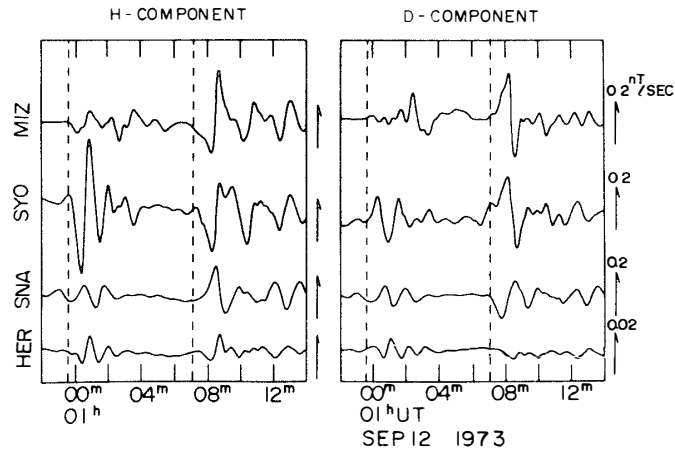


Fig. 17b. Band-pass filtered wave trains of the Pi pulsations observed over the wide area from the auroral region to the low latitude. The substorm expansions started at about 0100 and 0107 UT on September 12, 1973 (cf. Fig. 17a).

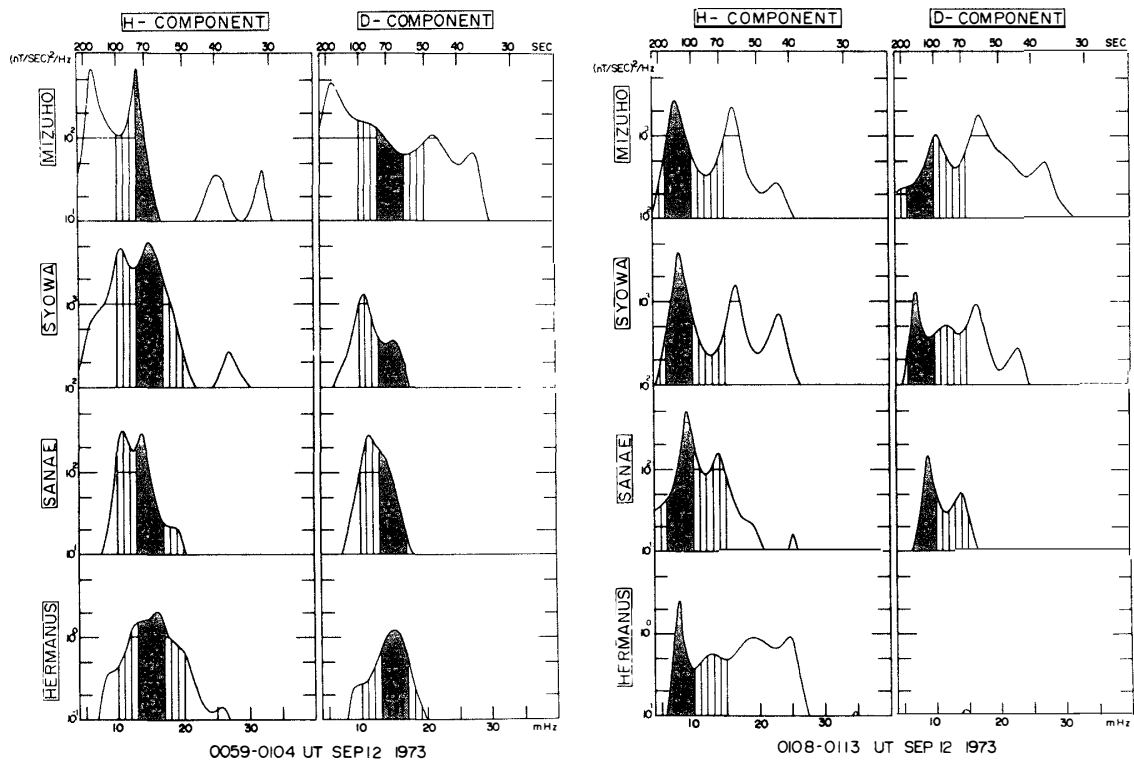


Fig. 17c. Power spectra calculated in the intervals of 0059–0104 and 0108–0113 UT on September 12, 1973, overlapping the data of Fig. 17b.

(-66.6°) to high(-68.0°) latitude in these two successive events. The band-pass filtered wave trains of the Pi pulsations are illustrated in Fig. 17b. The power spectra of those two successive Pi pulsations are computed in the intervals of 0059–0104 and 0108–0113 UT and shown in Fig. 17c. In the former event(0059–0104 UT), relatively dominant spectral components around 67 sec ($15 \text{ mHz} \pm 2 \text{ mHz}$) are observed concurrently at Syowa, Sanae and Hermanus. In the latter event(0108–0113 UT), the spectral peak is found around 120 sec($8\text{--}9 \text{ mHz}$). These spectral components will correspond to the Pi2's. In this multiple onset substorm, the location of auroral breakup shifted from low to high latitude, and the associated Pi2 periods varied from short(67 sec) to long(117 sec).

In the substorm event occurred on September 10, 1973, the onsets of the H-component decrease occurred successively at about 1838 and 1846 UT at both Syowa and Mizuho(Fig. 18a). Judging from the Z-component variations, the latitude of auroral breakup region are estimated to be approximately 67.5° and 70.5° , respectively. The wave trains are illustrated in Fig. 18b. The power spectra in the intervals of 1838–1843 and 1846–1851 UT are shown in Fig. 18c. Common peaks between Mizuho and Syowa are $\sim 77 \text{ sec}$

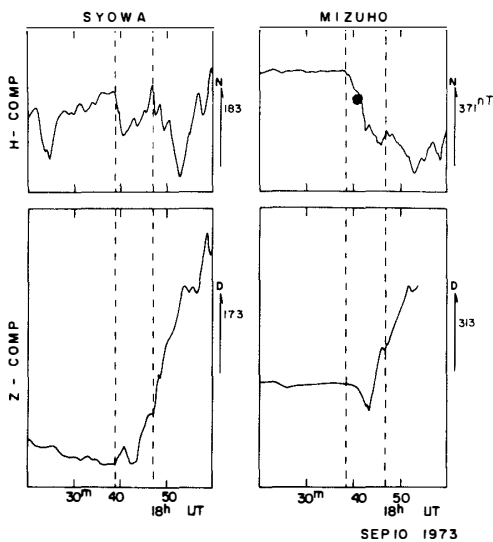


Fig. 18a. Magnetic variations of the H- and Z-components simultaneously observed at Mizuho and Syowa Stations on September 10, 1973. Two successive substorm expansions started at about 1838 and 1846 UT, respectively(vertical dashed lines).

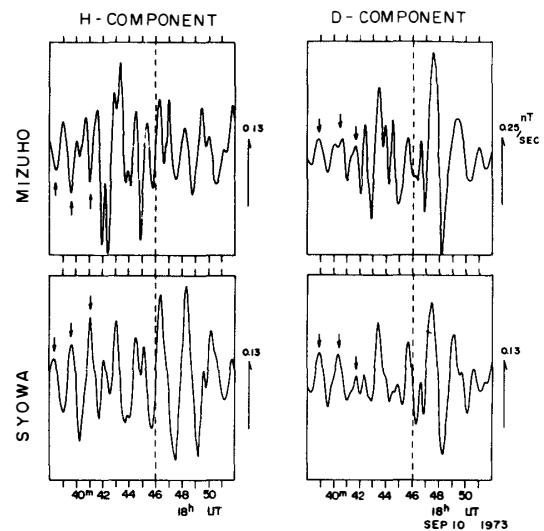


Fig. 18b. Band-pass filtered wave trains of the Pi pulsations. The substorm expansions started at about 1838 and 1846 UT on September 10, 1973(cf. Fig. 18a).

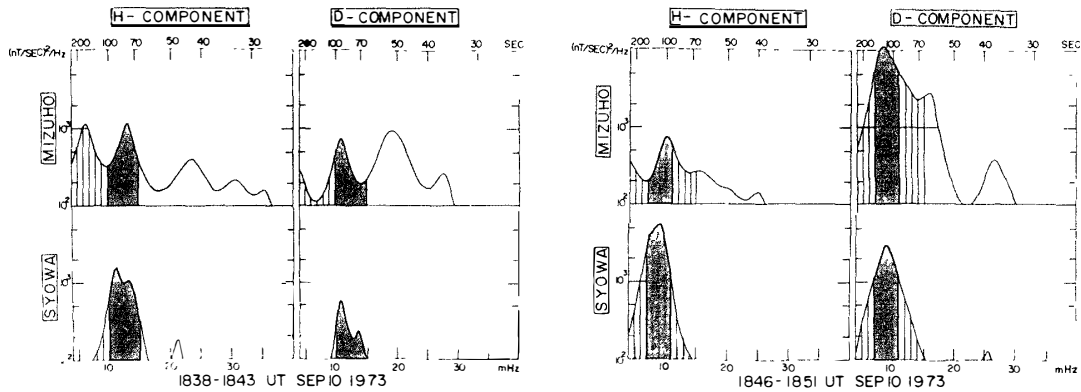


Fig. 18c. Power spectra calculated in the intervals of 1838–1843 and 1846–1851 UT on September 10, 1973, overlapping the data of Fig. 18b.

(~ 13 mHz) in the first event (1838–1843 UT) and ~ 110 sec (~ 9 mHz) in the second event (1846–1851 UT). Corresponding to a shift of the location of auroral breakup event from low to high latitude, the variation of the associated Pi2 period from short to long are found in this event too.

An systematic Pi2 period variation from short to long is also seen in an example shown in Figs. 19a and b. In this event, two successive Pi2's started at about 1822 and 1829 UT. Pi2 periods are ~ 45 sec in the first event (1822–1827 UT) and ~ 55 sec in the second event (1830–1835 UT), respectively.

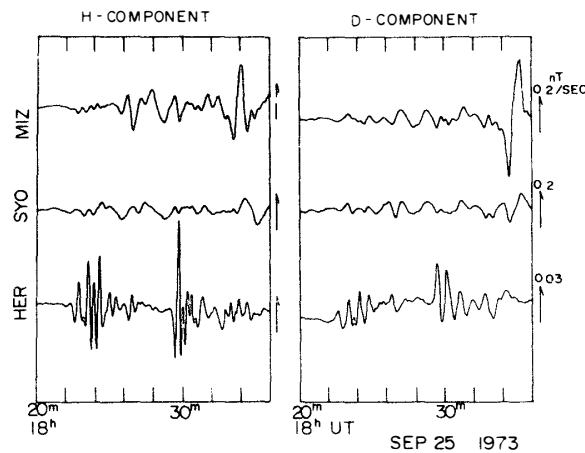


Fig. 19a. Band-pass filtered wave trains of the Pi pulsations over the wide area from the auroral region to the low latitude on September 25, 1973.

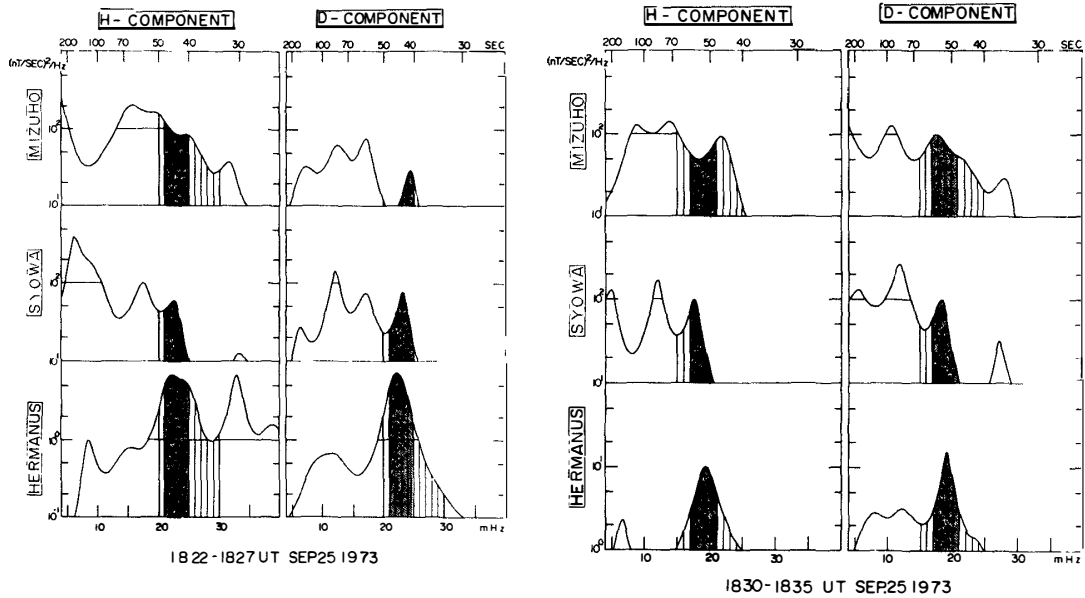


Fig. 19b. Power spectra calculated in the intervals 1822–1827 and 1830–1835 UT on September 25, 1973, overlapping the data of Fig. 19a.

In the multiple onset event, several breakups occurred successively within the interval of 10 minutes or so, while the instantaneous auroral breakup position shifted from low to high latitude systematically. In association with a shift of the auroral breakup position, the Pi2 periods vary from short to long.

4.4. Relationship between Pi2 period and latitude of auroral breakup region: Statistical study

In the section 4.2, a relation between Pi2 period and the latitude of auroral breakup region was studied on a non-statistical basis and it is suggested that the period of Pi2's associated with auroral breakup events occurred at higher latitudes is longer than the period of Pi2's associated with auroral breakup event occurred at lower latitude. In the section 4.3, the Pi2 period behaviors in the multiple onset substorm event were studied. And it is found that in association with the systematical shift of the location of auroral breakup region from low to high latitude, the associated Pi2 period also varies from short to long. In this section, the relationship between Pi2 period and location of auroral breakup event is studied on a statistical basis.

During the period from August 29 to September 29, 1973, ninety magnetic substorm events were observed at Syowa and at Mizuho. For the thirty-nine events, the geomagnetic latitudes of the occurrence region of auroral breakup events can be identified by the auroral data from Syowa

or the magnetic data from Syowa, Mizuho and Mawson. The method for estimation of the latitude of the auroral breakup region from magnetic data has been already given in Chapter 3.

The period of Pi2 is determined from the power spectra of Pi pulsations observed over the wide area in the expansion phase of the substorm. If a similar spectral component is seen over the wide area from the auroral region to low-latitudes ($f_0 \pm \Delta f$, Δf ; 1–2 mHz) this component is defined as the Pi2. If a dominant spectral component in the auroral region is somewhat different from that in lower latitudes stations, the dominant component in the auroral region is adopted as the Pi2 component in the present analysis. Among thirty-nine events whose auroral breakup position can be accurately determined, the Pi2 period for thirty-four events can be identified from the spectra. The result is shown in Fig. 20. In the figure the following close relation is evident that when the auroral breakup occurs at a higher(lower) latitude, the periods of the associated Pi2 becomes longer(shorter).

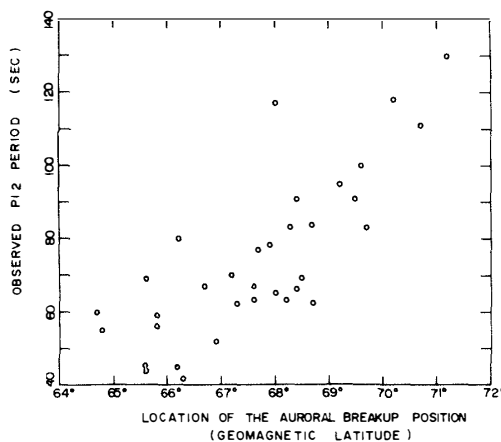


Fig. 20. Observed relations between the auroral breakup positions (in geomagnetic latitude) and the associated Pi2 periods.

4.5. Latitudinal dependence of Pi2 amplitude

Several research workers have shown that the Pi2 amplitude shows a primary maximum under the auroral electrojet (SAITO, 1969; OLSON and ROSTOKER, 1975) and a secondary one near the plasmopause (RASPOPOV *et al.*, 1972; SAITO *et al.*, 1976). In this section, latitudinal dependence of Pi2 amplitude is examined.

The latitudinal profile of Pi2 power intensities for the August 31, 1973 event (*cf.* Figs. 12a and b) is given in Fig. 21. In the figure, the powers are

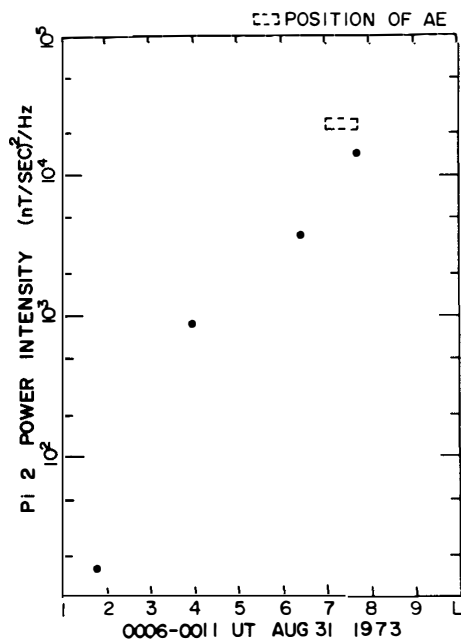


Fig. 21. Pi2 power intensities at Mizuho ($L=7.7$), Syowa ($L=6.3$), Sanae ($L=4.0$) and Hermanus ($L=1.8$) in the interval of 0006–0011 UT on August 31, 1973 (cf. Figs. 12a and b).

calculated for the horizontal component. The location at which the auroral breakup occurred is marked by a rectangle. It is evident that Pi2 power intensity is the largest in the neighborhood of the auroral breakup region. On the assumption that the Pi2 amplitude has a maximum at the auroral breakup region, the maximum power is estimated by a procedure which schematically

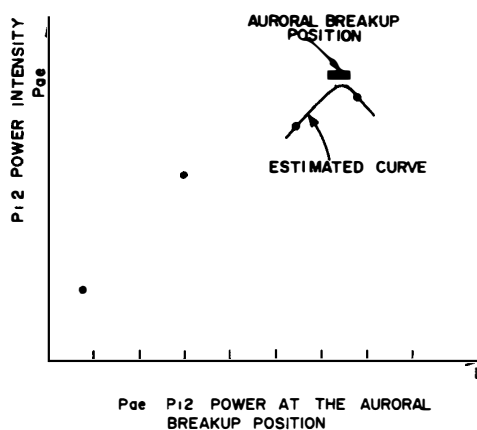
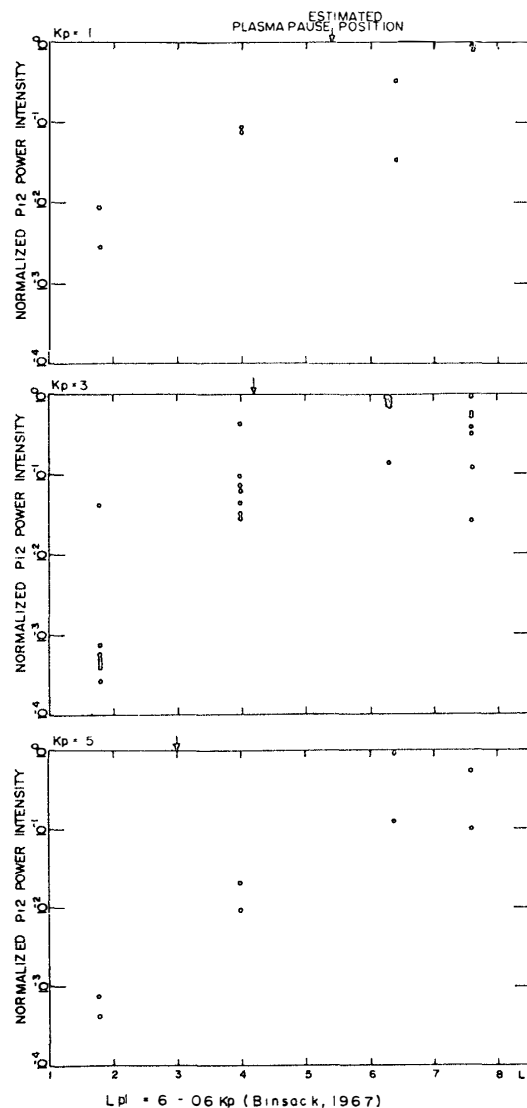


Fig. 22. Estimation method of the Pi2 power intensity (P_{ae}) under the auroral breakup position.

illustrated in Fig. 22. A parabola curve is determined so as to interpolate the values at Syowa and Mizuho, and to have a maximum (P_{ae}) at the auroral breakup region. P_{ae} is an estimated Pi2 power intensity at the auroral breakup region. Using this value (P_{ae}), the Pi2 power intensities at Syowa, Mizuho, Sanae and Hermanus are normalized. If an auroral breakup occurred at an observing station, the normalized value at that station is 1.0.

For the twenty-four substorm events in which auroral breakups occurred in the neighborhood of Syowa and Mizuho, the parabola curves and P_{ae} 's (*cf.* Fig. 22) are determined. The magnetic condition in the period of the substorm occurrence is classified using K_p index, in quiet ($K_p=1$), moderately disturbed ($K_p=3$) and disturbed ($K_p=5$) conditions, respectively. Normalized

Fig. 23. Normalized Pi2 power intensities at Mizuho ($L=7.7$), Syowa ($L=6.3$), Sanae ($L=4.0$) and Hermanus ($L=1.8$) during the quiet ($K_p=1$), moderately disturbed ($K_p=3$) and disturbed ($K_p=5$) conditions. Plasmapause positions are estimated from the following relation, $L_{pl}=6-0.6 K_p$ (BINSACK, 1967) and are marked by arrows in the figures.



Pi2 power intensities at Mizuho(L=7.7), Syowa(L=6.3), Sanae(L=4.0) and Hermanus(L=1.8) are shown in Fig. 23 in the quiet(upper part), moderately disturbed(middle part) and disturbed(bottom part) conditions, respectively.

In the quiet period($K_p=1$), Pi2 amplitudes are larger at Mizuho (L=7.7) than at lower latitude auroral station Syowa(L=6.3). On the other hand in the disturbed time($K_p=5$), Pi2 amplitudes are larger at Syowa than at Mizuho. If the Pi2 amplitude has a maximum at the auroral oval, this can be interpreted as the equatorward shift of the auroral oval with an increase of the geomagnetic activity and is consistent with the results by AKASOFU and CHAPMAN(1963), FELDSTEIN and STARKOV(1968).

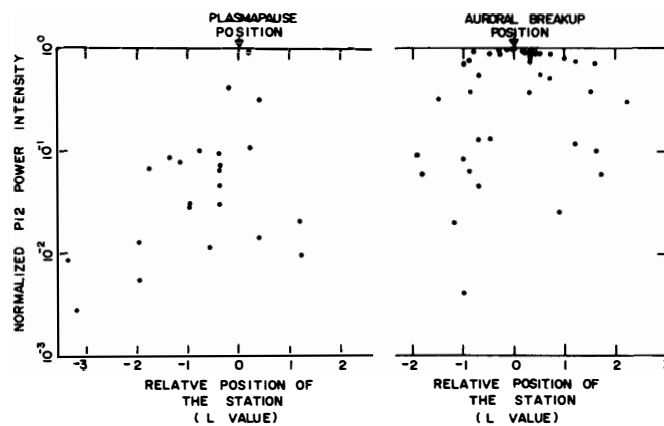


Fig. 24. Normalized Pi2 power intensities are plotted with relative position to the auroral breakup position at Mizuho and Syowa, whereas with relative positions to the plasmapause at Sanae and Hermanus.

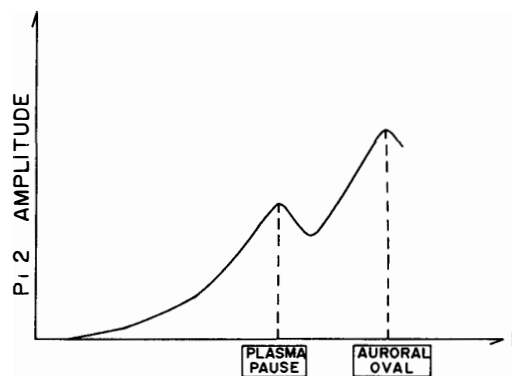


Fig. 25. Schematic profile of the latitude dependence of the Pi2 amplitude (cf. Fig. 24).

The averaged plasmopause position can be estimated by the following relation (BINSACK, 1967),

$$L=6.0-0.6 \cdot K_p$$

and the estimated plasmopause positions are given in Fig. 23. When the plasmopause is located in the neighborhood of Sanae(L=4.0), Pi2 amplitudes at Sanae become larger. This tendency is seen more clearly in Fig. 24. In the figure, the normalized Pi2 power intensity is plotted against the relative position to the auroral breakup position for the data at Syowa and Mizuho, whereas against the relative position to the plasmopause for the data at Sanae and Hermanus. It is evident from Fig. 24 that the Pi2 amplitude has a primary maximum at the auroral oval and a secondary one at the plasmopause. This relation is illustrated schematically in Fig. 25.

4.6. Summary of the spectral features of the Pi2

The spectral features of the Pi2 are summarized as follows.

(1) The Pi2 is observed simultaneously over the whole dark hemisphere of the earth's surface in coincidence with the onset of the substorm which is identified by a sharp H-component decrease and an onset of an auroral breakup event.

(2) The Pi2 amplitude shows characteristic latitude dependence. Its latitudinal profile shows a primary maximum near the auroral breakup region and a secondary one near the plasmopause.

(3) The Pi amplitude is not necessarily proportional to a magnitude of the auroral electrojet. Pi2 events are distinctly observed over the wide area even when the associated magnetic substorms are small.

(4) The Pi2 period is closely associated with the latitude of the auroral breakup region. When the auroral breakup occurs at a higher(lower) latitude, the Pi2 period becomes longer(shorter).

(5) In the multiple onset substorm events, the auroral breakup occurs at a lower latitude at first, then the next breakup occurs at a higher latitude. With the systematical shift of the auroral breakup region from low to high latitude, the period of associated Pi2 pulsations varies from short to long one.

5. Polarization of the Pi2 Pulsations

As is found in the previous chapter, the latitude dependence of the Pi2 amplitude shows a primary maximum in the auroral region and a secondary one near the plasmopause. This fact indicates that Pi2 pulsations are primarily generated in the auroral breakup region. The role of the auroral breakup in the generation and propagation of Pi2's will be made clear by studying polarization characteristics of Pi2's observed in the auroral region.

5.1. Spatial distribution of Pi2 polarization in the auroral region

Successive Pi2 events in a substorm are considered as independent phenomena in this analysis. The local time dependence of Pi2 occurrence is given in Fig. 26. The figure shows a primary maximum in the Pi2 occurrence around 2100–2200 MLT and a secondary one around 0000–0100 MLT. The occurrence peak around 2100–2200 MLT is consistent with that reported previously (*e.g.*, KATO *et al.*, 1956; YANAGIHARA, 1960).

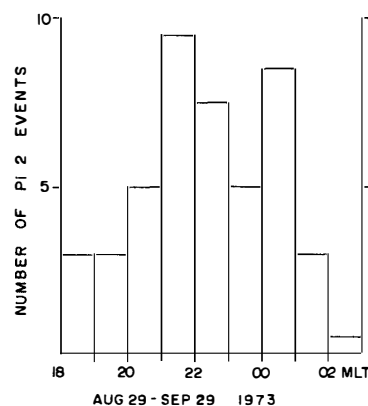


Fig. 26. Magnetic local time dependence of Pi2 occurrences during the period from August 29 to September 29, 1973.

the poleward side of Mizuho(68.7°) around 2250 UT(MLT) on September 1, 1973. This event occurred after the time of the Pi2 maximum occurrence. The estimated geomagnetic latitude of the auroral electrojet is about 69.5° . Associated with this auroral breakup, Pi2 with a damped type waveform was observed(Fig. 14b). As shown in Fig. 14b, both H- and D-components oscillate almost in phase at Mizuho and at Syowa. Hodograms in the H-D plane plotted in the interval of 2251–2253 UT are illustrated in Fig. 28. The hodograms show right-hand polarizations(counterclockwise) at both Syowa and Mizuho. It is also apparent in the figure that the polarization at Mizuho is almost linear and its major axis is oriented in the north-east direction, while the polarization at Syowa is close upon circular. In this event, the location of the auroral breakup region is nearer to Mizuho than to Syowa.

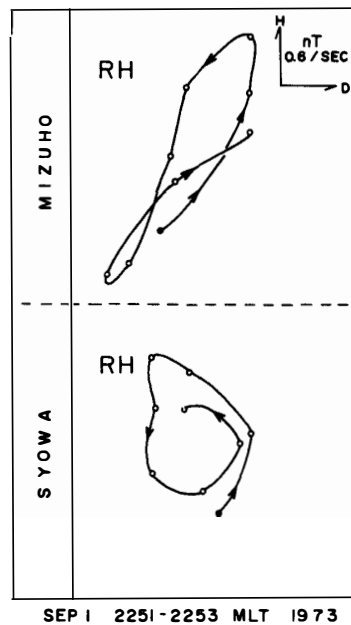


Fig. 28. Wave hodograms of the Pi2 component in the horizontal plane. Open circles in each hodogram correspond to every 15 sec intervals. The RH represents right-hand polarization.

Fig. 29 shows the hodogram of the event which occurred around 2112 UT on September 17, 1973. The estimated geomagnetic latitude of the auroral breakup region is about 70.5° . The wave hodograms of the horizontal plane show the left-hand polarizations(clockwise in the southern hemisphere) at the two stations. The sense of polarization is opposite to that of the previous event. This event occurred before the time of the Pi2 maximum occurrence.

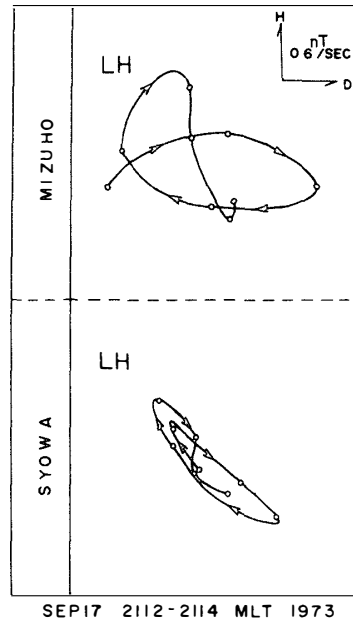


Fig. 29. Wave hodograms of the Pi2 component in the horizontal plane. Open circles in each hodogram correspond to every 15 sec intervals. The LH represents left-hand polarization.

5.3. Polarization characteristics of Pi2 pulsations observed in a poleward region of the auroral breakup region

All-sky photographs in Figs. 15a and b and simultaneous magnetic records show that an auroral breakup occurred on an equatorward side of Syowa at about 2354 UT on September 10, 1973. This event occurred after the time of the Pi2 maximum occurrence. Polarization hodograms plotted in the interval of 2356–2358 UT are illustrated in Fig. 30. At Syowa, the left-hand polarized waves are predominant. At Mizuho, though the polarization is somewhat complicated, the left-hand polarization seems to be predominant, too.

Fig. 31 shows another example of Pi2 event observed poleward of the auroral breakup region. From the magnetic records illustrated in Fig. 11a, it is found that the auroral breakup occurred on a little equatorward side of Syowa at about 2020 UT. This event occurred before the time of the Pi2 maximum occurrence. The wave hodograms plotted for the H-D plane in the interval of 2021–2023 UT are illustrated in Fig. 31. At Syowa, right-hand polarized waves (counterclockwise) are predominant, whereas at Mizuho, the polarization is very complicated and its sense is uncertain in this case.

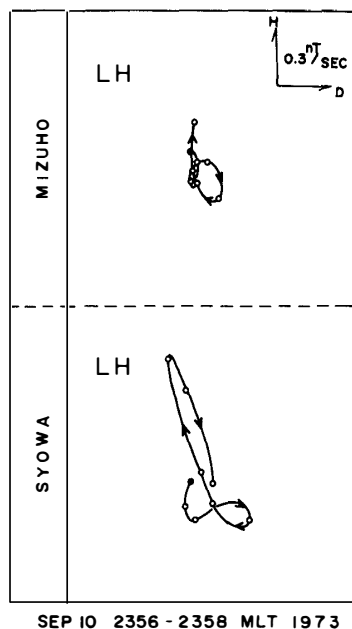


Fig. 30. Wave hodograms of the Pi2 component in the horizontal plane. Open circles in each hodogram correspond to every 15 sec intervals. The LH represents left-hand polarization.

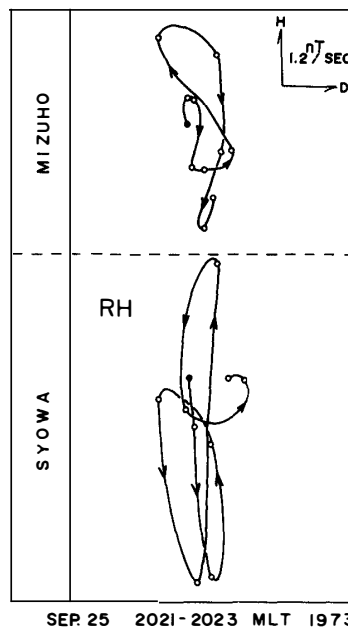


Fig. 31 Wave hodograms of the Pi2 component in the horizontal plane. Open circles in each hodogram correspond to every 15 sec intervals. The RH represents right-hand polarization.

5.4. Polarization characteristics of Pi2 pulsations when the associated auroral breakup event occurred between Syowa and Mizuho

Judging from the magnetic variations of the Z-component at Mizuho and Syowa, it is suggested that the auroral breakup in the September 5, 1973 event occurred between Mizuho and Syowa. The band-pass filtered wave trains are illustrated in Fig. 32a for H- and D-components. In the figure, the waveforms are similar at both stations. However, the wave phase relation shows a drastic difference between Mizuho and Syowa. The D-components oscillated almost in phase between the two stations, whereas the H-components oscillated almost out of phase. This large phase shift of the H-component gives rise to the polarization reversal across the auroral breakup region as shown in the hodograms plotted in the interval of 2026–2028 UT in Fig. 32b. The left-hand polarization (clockwise) is predominant at Syowa which is located equatorward of the auroral breakup region, while the right-handed (counterclockwise) one is seen at Mizuho which is located poleward of the auroral breakup region. This event occurred before the time of the Pi2 maximum occurrence.

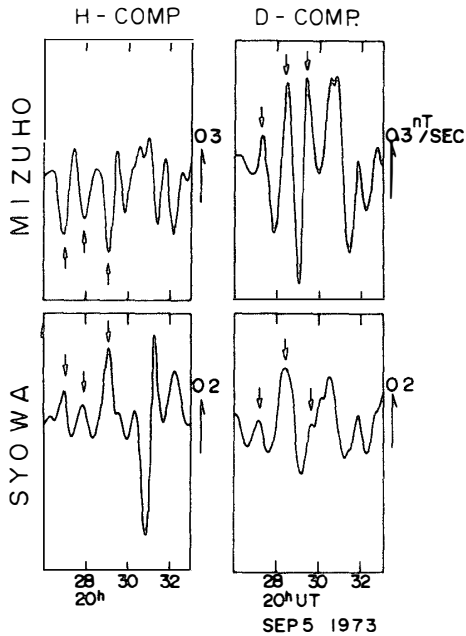


Fig. 32a. Band-pass filtered wave trains of the Pi2. The auroral breakup occurred at the region between Mizuho and Syowa at about 2026 UT on September 5, 1973. H-component oscillated out-of phase, whereas D-component oscillated in-phase between the two stations.

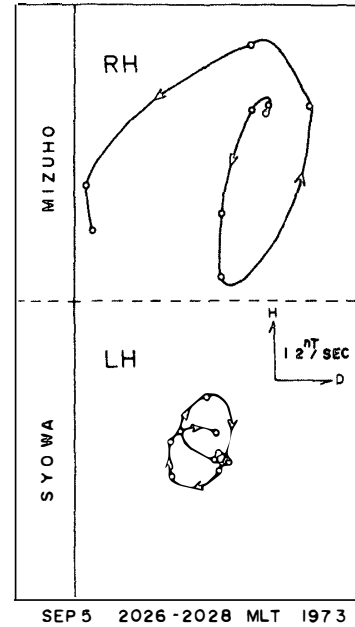


Fig. 32b. Wave hodograms of the Pi2 component in the horizontal plane. Open circles in each hodogram correspond to every 15 sec interval. The RH and LH represent right-hand and left-hand polarization, respectively.

The September 10, 1973 event given in Figs. 18 and 33 occurred also before the time of Pi2 maximum occurrence. The onsets of substorms occurred at about 1838 and 1846 UT, successively. The former breakup event occurred between Mizuho and Syowa, while the latter breakup event occurred on a poleward side of the two stations (Fig. 18a). In association with each onset of the auroral breakup, the intensifications of the Pi2 were observed at about 1838 and 1846 UT, respectively (Fig. 18b). In the first event whose associated substorm breakup occurred between Mizuho and Syowa, the Pi2 waves oscillated almost out of phase in the H-component, whereas almost in phase in the D-component at the two stations. In the second event whose associated breakup occurred on a poleward side of both stations, the Pi2 waves oscillated almost in phase in each component at the two stations. For the first events, the polarization hodograms are plotted in the interval of 1838–1840 UT in Fig. 33. At Syowa, the left-hand polar-

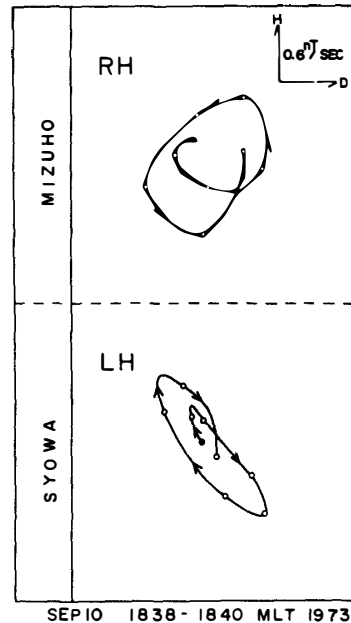


Fig. 33. Wave hodograms of the Pi2 component in the horizontal plane. Open circles in each hodogram correspond to every 15 sec interval. The RH and LH represent right-hand and left-hand polarization, respectively. The auroral breakup occurred at the region between Mizuho and Syowa at about 1838 UT on September 10, 1973 (cf. Figs. 18a and b).

ized wave is found, whereas at Mizuho, the Pi2 wave is clearly right-hand polarized. The sense of Pi2 polarization reversed across the auroral breakup region.

The auroral breakup occurred at a midway between Mizuho and Syowa at about 2152 UT on September 22, 1973. The wave hodograms plotted in the interval of 2152–2154 UT show complicated polarization behaviors at both stations (Fig. 34). However, it is found that the right-hand polarization (counterclockwise) is predominant at Syowa, while the left-hand polarization (clockwise) predominates at Mizuho, respectively. Pi2 polarization reversal across the auroral breakup position is also found in this event, too. However, the process of Pi2 polarization reversal is opposite to the previous two examples. This event occurred after the time of the maximum Pi2 occurrence.

In this section, Pi2 polarization characteristics across the auroral oval are investigated with 3 typical events on a non-statistical basis. So far as these typical phenomena are concerned, Pi2 polarization reversal occurs across the auroral oval where Pi2 amplitude shows a major maximum, and also across around 2100–2200 MLT where Pi2 occurrence frequency becomes maximum

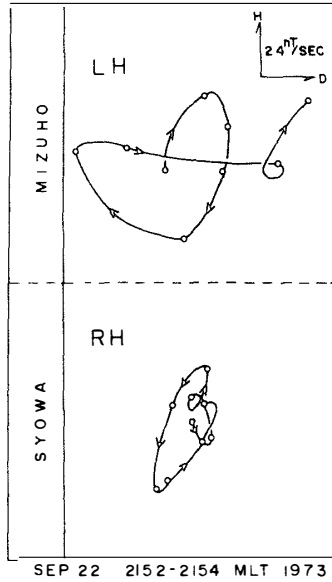


Fig. 34. Wave hodograms of the Pi2 component in the horizontal plane. Open circles in each hodogram correspond to every 15 sec interval. The RH and LH represent right-hand and left-hand polarization, respectively. The auroral breakup occurred at the region between Mizuho and Syowa at about 2152–2154 UT on September 22, 1973.

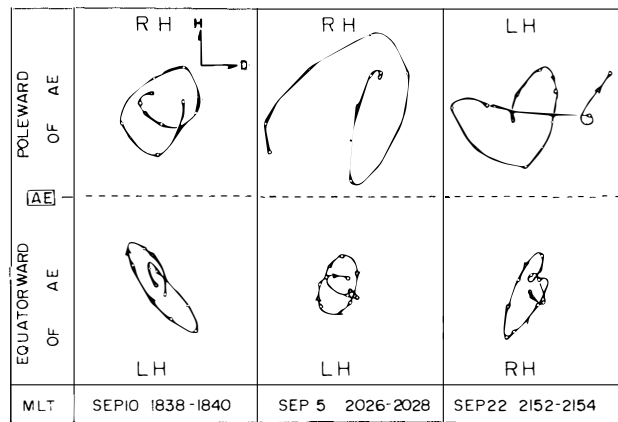


Fig. 35. Wave hodograms of the Pi2 component shown in Figs. 32b, 33 and 34 are summarized.

(Fig. 35). The polarization reversal is due to the 180° phase shift of the H-component across the auroral oval.

5.5. Pi2 polarization characteristics across the auroral breakup region: Statistical study

The polarization reversal of Pi2 pulsation across the auroral breakup region as well as across the time of the Pi2 maximum occurrence is found on a non-statistical analysis in the sections 5.2.–5.4. In this section, this problem is examined on a statistical basis.

Among ninety Pi2 events shown in Fig. 26, locations of the observing stations to the auroral breakup region (equatorward? or poleward?) can be identified for the seventy-eight events. The sense of polarization of these seventy-eight Pi2 events is given in Fig. 36. It can be stated from the figure that the Pi2 polarization observed at a poleward station of the auroral breakup region is right-handed before the time of the Pi2 maximum occurrence and left-handed thereafter. At an equatorward station, on the other hand, the observed Pi2 polarization is left-handed before the time of the Pi2 maximum occurrence and right-handed thereafter. In order to show clearly these Pi2 polarization characteristics, occurrence frequencies of right-hand and left-hand polarization are shown by the percentage in Fig. 37. The above mentioned Pi2 polarization reversals are clearly represented in the figure.

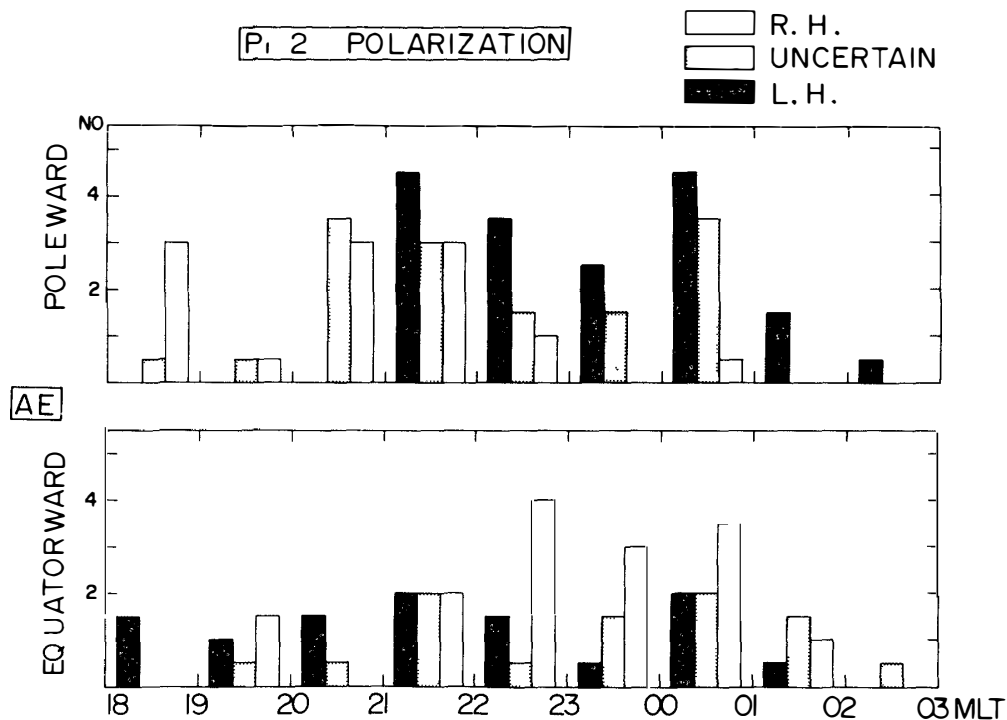


Fig. 36. Magnetic local time dependences of the polarization of the Pi2 disturbance vector on the poleward side and on the equatorward side of the auroral breakup position.

Wave Characteristics of Magnetic Pi2 Pulsations

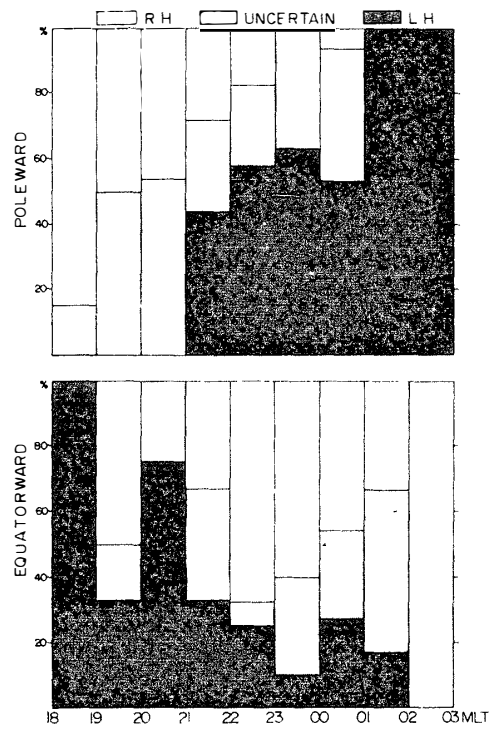


Fig. 37. Magnetic local time dependences of the polarization of the Pi2 disturbance vector on the poleward side and on the equatorward side of the auroral breakup position (Representation in Fig. 36 is arranged in the occurrence probability).

6. Conjugate Relationship of Pi2 Pulsations

The conjugacy of Pi2 pulsations in the auroral region is examined on the basis of the simultaneous data observed at Syowa Station and Reykjavik. These two stations are the best conjugates-pair stations among many stations located in the auroral region. Their corrected geomagnetic coordinates are $-66.7^\circ, 72.4^\circ$ ($L=6.3$) at Syowa and $66.6^\circ, 71.2^\circ$ ($L=6.3$) at Reykjavik.

6.1. Example of Pi2 pulsations simultaneously observed at Syowa and Reykjavik

Statistical study of the Pi2 at subauroral-zone stations (New Zealand stations) in the southern hemisphere indicates that the polarization sense is opposite to that at the conjugate stations (Canadian stations) in the northern hemisphere (ROSTOKER, 1967; CHRISTOFFLE and LINFORD, 1966). This fact means that sense of the polarization along the geomagnetic line of force is the same in both the hemisphere. On the basis of the data obtained at the conjugate pair stations near the plasmopause ($L \approx 4$) FUKUNISHI (1975) showed that 23 of the 32 Pi2 events have odd mode symmetry characteristics. However, the conjugacy of Pi2 pulsations in the auroral region has been little reported up to the present.

In the present investigation, the rapid-run magnetograms of the H- and D-components obtained at Syowa and Reykjavik are digitized, at every 6 sec interval. Those digital data are high-pass filtered to pick up Pi2 waveforms from the original magnetic variations. The high-pass filter used here is a Gaussian type filter. Cut-off frequency with -3 dB is 5 mHz (200 sec). An example is illustrated in Fig. 38. In the figure, a sharp decrease of the H-component started almost simultaneously at Syowa and Reykjavik at about 0008 UT on September 17, 1973. Their minimum values of the H-component decreases are -270 nT at Syowa and -212 nT at Reykjavik, respectively. It is also detectable in the figure that the magnetic oscillations overlapped on the negative changes at both stations. These components in this event are

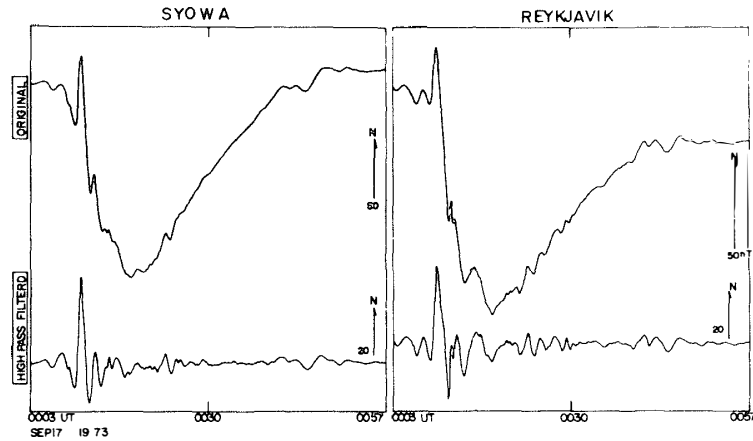


Fig. 38. Original and high-pass filtered magnetograms of the H-components simultaneously observed at the conjugate stations (Syowa and Reykjavik) on September 17, 1973.

picked up by means of the digital high-pass filtering technique and shown in the lower part of Fig. 38.

This Pi2 component is compared with the simultaneous waveform observed by means of the induction magnetometer (Fig. 39). It is obvious from

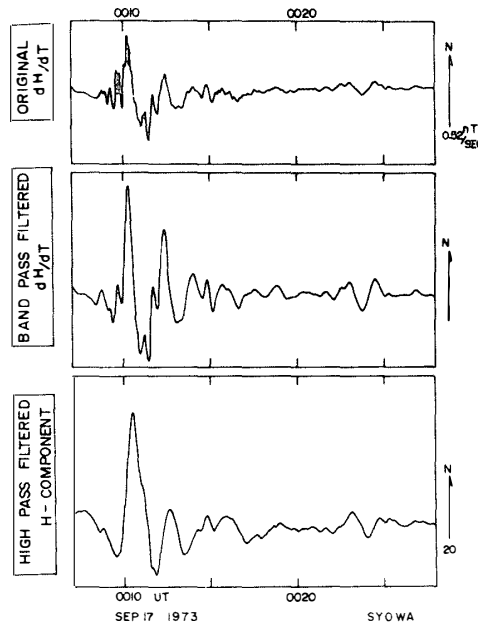


Fig. 39. Comparison of the waveforms of the original induction magnetogram (upper), the band-pass filtered induction magnetogram (middle) and the high-pass filtered rapid-run magnetogram (bottom).

the figure that the Pi2 waveform obtained by means of the rapid-run magnetometer(bottom part) has a common fundamental period component to the waveform obtained by means of the induction magnetometer(middle part), although the systematic 90° phase shifts for each component exist due to the differential effect of the induction magnetometer. The results shown in Fig. 39 indicates that the rapid-run magnetometer record is useful for studying Pi2 pulsations.

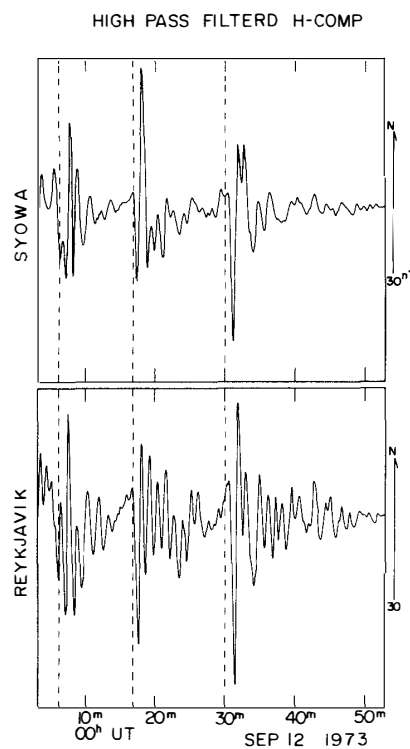


Fig. 40. High-pass filtered magnetograms of the H-component simultaneously observed at Syowa and Reykjavik on September 12, 1973.

A similar example to that shown in Fig. 38 is illustrated in Fig. 40. The onsets of three substorm occurred successively at about 0006, 0017 and 0031 UT on September 12, 1973(cf. Fig. 8). In association with these onsets, three individual Pi2 events are clearly seen on the high-pass filtered H-component magnetograms at the conjugate-pair stations. It is obvious from the figure that in association with the substorm expansion, the similar Pi2 wave trains are simultaneously observed at the conjugate stations.

6.2. Pi2 polarization characteristics at conjugate-pair stations:Case study

Wave phase relations and polarization characteristics of Pi2 pulsations at the conjugate-pair station are examined for several typical events.

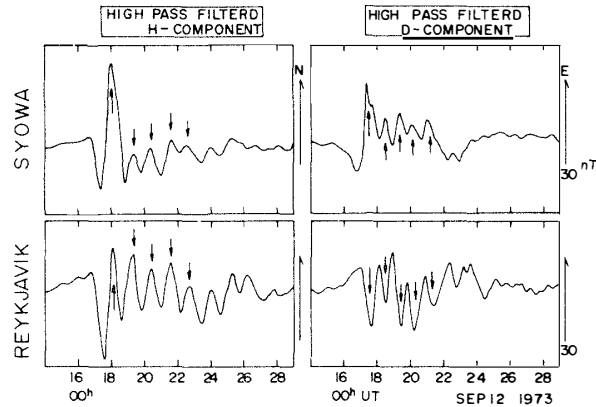


Fig. 41a. Enlarged high-pass filtered magnetograms of the H-component, overlapping the data of Fig. 40.

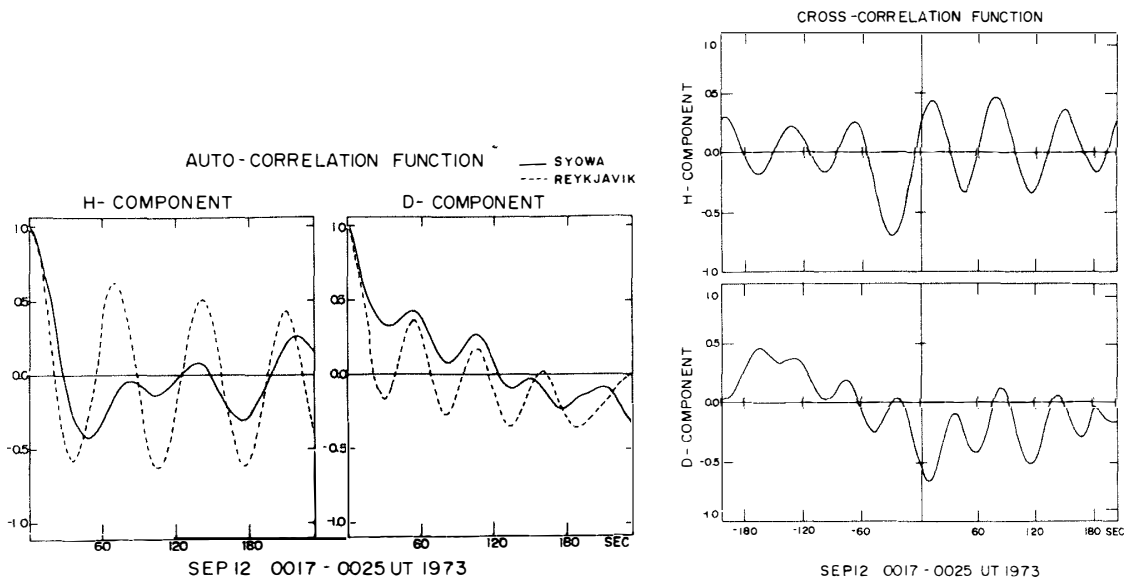


Fig 41b. Auto- and cross-correlation functions of the high-pass filtered H- and D-components simultaneously observed at Syowa and Reykjavik, overlapping the data of Fig. 41a

Fig. 41a shows the enlarged high-pass filtered magnetograms for the second event in Fig. 40(Fig. 41). Judging from the Z-component variations, it is suggested that the auroral breakup occurred on a poleward side of both stations. In Fig. 41a, the H-components show almost in-phase oscillations, whereas the D-component show almost out-of-phase oscillations at the conjugate-pair stations. In Fig. 41b, auto-correlation functions for the H- and D-components at Syowa and Reykjavik, as well as cross-correlation functions between the two stations are illustrated. The auto-correlation functions show similar shapes at Syowa and Reykjavik for both the H- and D-components, indicating that the Pi2 oscillates with almost the same period at the

conjugate-pair stations. On the other hand, the cross-correlation functions show a difference between the H- and D-components. The H-component shows a positive correlation with a maximum of 0.43, whereas the D-component shows a negative correlation with a maximum of -0.65 .

Another example of Pi2 event associated with a small-scale substorm is given in Figs. 42a and b. Judging from the Z-component magnetograms from Syowa, Mizuho and Mawson, it is suggested that the auroral breakup occurred near Mawson at about 0040 UT. In a case of the small magnetic substorm, irregular component caused by ionospheric current may be small. In association with this substorm event, Pi2 pulsations were observed simultaneously at the conjugate points and their high-pass filtered waveforms are traced in Fig. 42a. The H-components oscillated almost in-phase and the D-components oscillated almost out-of-phase at the conjugate-pair station. The cross-correlation functions in Fig. 42b show a positive correlation in the H-component with a maximum of 0.92, and a negative correlation in the D-component with a maximum of -0.70 , respectively. The hodograms in the H-D plane are illustrated in Fig. 42c. In the figure, the right-hand polarization(counter-clockwise in the southern hemisphere) is seen at Syowa, and the right-hand polarization(clockwise in the northern hemisphere) is also seen at Reykjavik. The major axis is oriented in the north-west direction at Syowa, while it is oriented in the north-east direction at Reykjavik. The hodogram at Syowa is symmetrical about the meridian plane to that at Reykjavik.

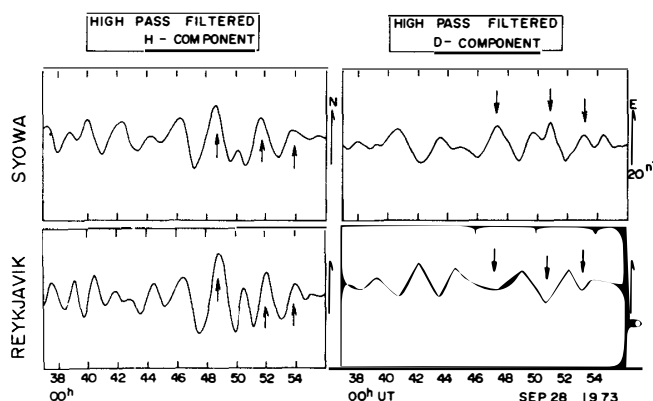


Fig. 42a. Enlarged high-pass filtered magnetograms of the H- and D-components simultaneously observed at Syowa and Reykjavik on September 28, 1973.

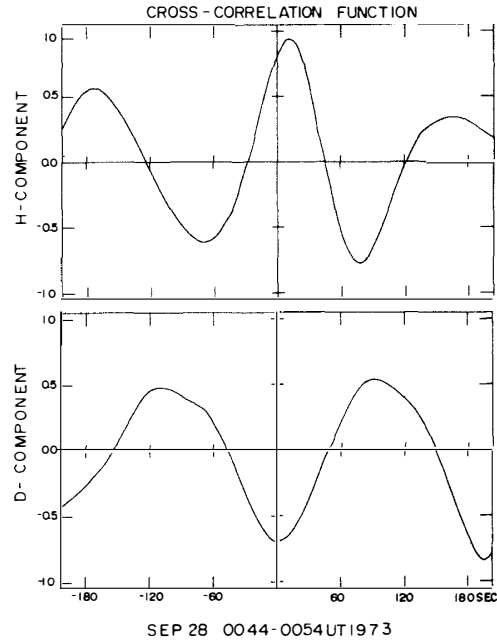


Fig. 42b. Cross-correlation functions of the H- and D-components, overlapping the data of Fig. 42a.

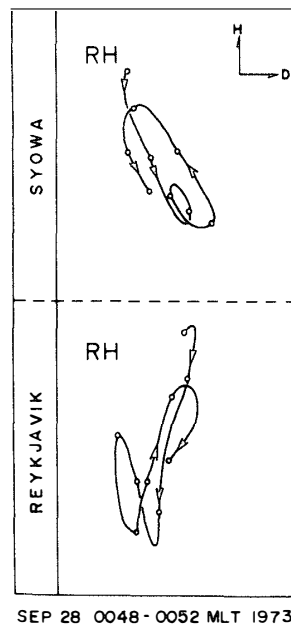


Fig. 42c. Wave hodograms of the Pi2 component in the horizontal plane, overlapping the data of Fig. 42a.

6.3. Pi2 polarization characteristics at conjugate-pair stations: Statistical study

During the period of August 29 to September 29, 1973, ten Pi2 events

were simultaneously recorded at Syowa and Reykjavik. For these ten events, the wave phase differences of the H- and D-components between the two stations were determined from the auto- and the cross-correlation functions. The result is given in Fig. 43. The figure shows that the H-components oscillate almost in-phase, whereas the D-components oscillate almost out-of-phase in the conjugate regions.

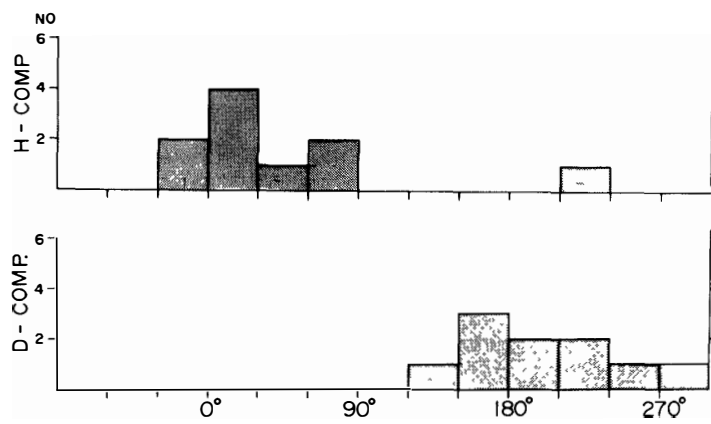


Fig. 43. Wave phase differences of the H- and D-components of the Pi2 between Syowa and Reykjavik.

7. Discussion

7.1. Interpretation of wave phase relations of Pi2 pulsations at conjugate-pair stations

The Pi2 wave phase relation between the conjugate-pair stations can be interpreted by an idealized elastic string model of SUGIURA and WILSON (1964). Their model has shown the symmetry relations in the magnetic perturbation at a pair of conjugate points due to the oscillation of the line of forces of the geomagnetic field. The model is illustrated in Fig. 44. This model, although obviously oversimplified for field line configuration in the magnetosphere, nevertheless gives a geometrical picture of a field line oscillation.

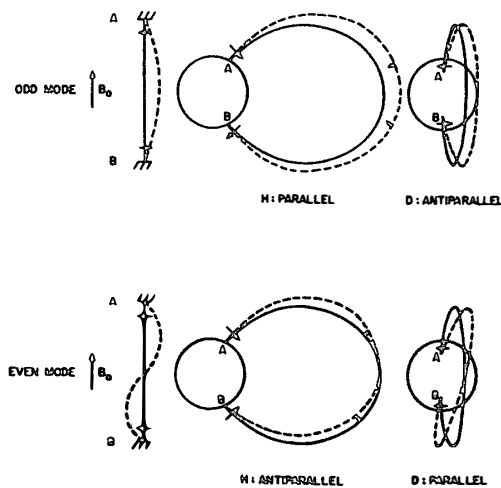


Fig. 44. The symmetry relations at magnetically conjugate points for oscillation of the lines of magnetic force. H , horizontal component. D , east declination. Arrow, magnetic perturbation. (After SUGIURA and WILSON, 1964).

tion. The model requires the following assumption that the cold plasma distribution and the magnetic field configuration is symmetric with respect to the magnetic equator. These assumptions are satisfied in the magnetosphere with phenomena having a sufficiently long wavelength like as Pi2 pulsations.

In the model shown in Fig. 44, the magnetic perturbation is proportional to the derivative of the field line displacement and not to the displacement. For a two-dimensional model with Z along the string (fixed at the two ends $Z=\pm a$) and the displacement $\xi_x(Z, t)$ measuring the displacement,

$$b_x = B_0 \frac{\partial \xi_x}{\partial Z},$$

where B_0 is the magnitude of the unperturbed field and b_x is the X component of the perturbation. For odd modes, the midpoint ($Z=0$) is a nodal point for b_x , where the magnitude of the displacement is a maximum there. For even modes b_x is a maximum at the midpoint. At the two ends, $Z=\pm a$, the sign of b_x is opposite for odd modes and the same for even modes. Applying the above relations to the geomagnetic field line, the following conclusions on the symmetry relations are drawn. For oscillations of odd modes, the H-component oscillates in-phase and the D-component oscillates out-of-phase at the conjugate-pair stations, whereas for even modes the H-component oscillates out-of-phase and the D-component oscillates in-phase at the conjugate points. Hence in the former case, the polarizations (as viewed downward) at the conjugate points are mirror images to each other with respect to the meridian plane, and in the latter case, they are mirror images with respect to the equator.

Pi2 polarization characteristics given in Fig. 43 suggest that Pi2 pulsations in the auroral region are odd mode standing oscillations.

7.2. Interpretation of dominant periods in Pi2 pulsations

Relations between periods of Pi2 pulsations and the geomagnetic activities have been investigated by many research workers using K_p index, magnitude of the associated bay, and others. The predominant period of Pi2 pulsations becomes short when K_p increases (TROITSKAYA, 1967; ROSTOKER, 1967; FUKUNISHI and HIRASAWA, 1970; SAITO and SAKURAI, 1970; CHANNON and ORR, 1970; DOBOV and MAINSTONE, 1973; STUART and BOOTH, 1974; SUTCLIFFE, 1975b). TROITSKAYA (1967) showed the monotonous decrease of Pi2 period with increase of the solar wind velocity. SAITO and MATSUSHITA (1968) investigated a relation between the period of Pi2 and the magnitude of the accompanying bay disturbance on the basis of the rapid-run magnetograms obtained at Fredericksburg and showed the following relation,

$$T = 163 (\sqrt{\Delta H^2 + \Delta D^2})^{-0.219} .$$

This results show that the Pi2 period decreases with increasing geomagnetic activity.

On the other hand, the location of the auroral oval also depends greatly on the geomagnetic activity. The average latitude of the equatorward boundary of the auroral oval in the midnight sector is higher than 70° in geomagnetic latitude under a very quiet period, while it shifts equatorward with increase of the magnetic activity and descends to as low as 50° during an intense magnetic disturbance (AKASOFU and CHAPMAN, 1963; STRINGER *et al.*, 1965; STRINGER and BELON, 1967; FELDSTEIN and STARKOV, 1968). From these results, the Pi2 period seems to be closely related to the latitude of the auroral oval.

SAITO and SAKURAI (1970) suggested that the Pi2 source region is closely related to the position of the inner boundary of the plasmashet from the close correlation between the equatorial distance of the inner boundary of the plasmashet and the Pi2 intensity maximum region (Fig. 9 of SAITO and SAKURAI, 1970). In the present analysis, it is found that when the auroral breakup occurs at a higher(lower) latitude, the associated Pi2 period becomes longer(shorter) (*cf.* Fig. 19). These results indicate that the Pi2 source region is located in the auroral breakup region.

A main cause of the Pi2 is thought to be the torsional oscillations of field lines passing through the auroral breakup region, as suggested by several research workers (SAITO and SAKURAI, 1970; SAKURAI, 1970; ROSTOKER, 1967; STUART and BOOTH, 1974; SAITO *et al.*, 1976). This is also supported by the following observational facts.

(1) Pi2's with similar waveforms are simultaneously observed at the conjugate stations in the auroral region, *e.g.* at Syowa and at Reykjavik.

(2) The latitude dependence of the Pi2 amplitude shows a primary maximum at the auroral oval and a secondary one at the plasmopause.

In order to check upon this model, we will compare periods of the torsional oscillation of the field line connected to the auroral oval with the observed Pi2 period. The wave period depends on the extent of the line of force, plasma density of the medium and its mode of oscillation. From the conjugate relationship of Pi2 wave phase, it is concluded that the mode of the Pi2 is an odd mode (*cf.* Fig. 43). The period of a torsional standing wave will be approximately the same as the bounce period of the wave packet (DUNGEY, 1954; ODAYASHI and JACOBS, 1958; WATANABE, 1961; JACOBS, 1970). The fundamental period T of the oscillating magnetic lines of force is given by the following integration along a geomagnetic line of force.

$$T = 2 \int_S \frac{dS}{V_A} \tag{7}$$

where $V_A = B/\sqrt{4\pi\rho}$ is Alfvén velocity, B is strength of local magnetic field and ρ is local plasma density.

Many research workers calculated the eigen period of the torsional oscillations for the investigation of the various magnetic pulsations (DUNGEY, 1954; OBAYASHI and JACOBS, 1958; WATANABE, 1961; WESTPHAL and JACOBS, 1962; CUMMINGS *et al.*, 1969; ORR and MATTHEV, 1971). Their calculated fundamental period of torsional oscillations are considerably long comparing with the observed Pi2 period. Recently, SAITO and SAKURAI (1976, Fig. 7) calculated the eigen period of the torsional oscillation in the case of a dipole field and variable plasma density distribution as given by CHAPPELL (1972) and showed how those periods to vary with latitude. We also calculated the eigen period of the field line oscillations under the circumstances of the dipole field for B , the gyro-frequency model for ρ and proton-electron plasma. The fundamental period of the torsional oscillation is given by

$$T = \frac{4R_E}{V_{AE}} \int_{\theta_0}^{\pi/2} \sin^4\theta \cdot (1 + 3\cos^2\theta)^{1/4} d\theta \quad (8)$$

where R_E is a distance of equatorial crossing of the line of force, V_{AE} is Alfvén velocity at the equatorial plane and θ_0 is a co-latitude of intersection of line of force on the Earth's surface. Those relation is illustrated schematically in Fig. 45.

The cold plasma density on the equatorial plane in the nightside is given from a smoothed profile deduced from CHAPPELL's (1972) measurement as

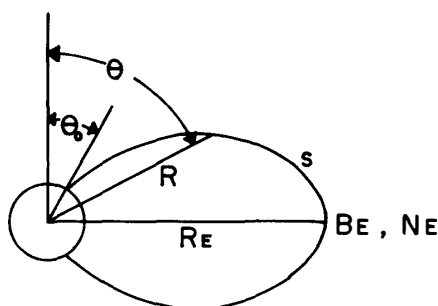


Fig. 45. Geometry of the geomagnetic lines of force. θ_0 , co-latitude of intersection of the magnetic line of force with the Earth's surface. R_E , geocentric distance of equatorial crossing of the magnetic line of force.

is shown in Fig. 46. Outside the plasmasphere the density profile is not affected by magnetic disturbance conditions. In the present plasma model, the density in the equatorial plane at $L=8$ is equal to $1.0/\text{cm}^3$. The magnetic field strength in the dipole field decreases monotonically with increasing latitude. Thus, a sharp change of the Alfvén velocity is expected around the plasmapause due to a sudden decrease of the plasma density. On the basis of the above situations, the fundamental period of the torsional oscillations were calculated and the results are illustrated in Fig. 47. In the figure, the periods in the auroral region ($65^\circ - 70^\circ$ in geomagnetic latitudes) range from 30 sec to 130 sec. The result is in agreement with the observed Pi2 period. It is also obvious in Fig. 47 that similar resonance periods as those in the auroral region will be also excited around the plasmapause. The calculated periods for the auroral latitudes are compared with the observed

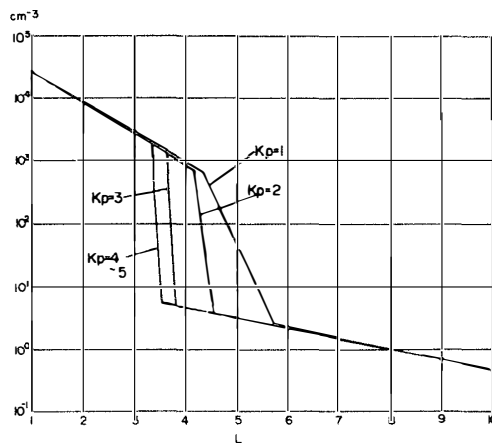


Fig. 46. Estimated plasma density profiles at the equatorial plane in the nightside.

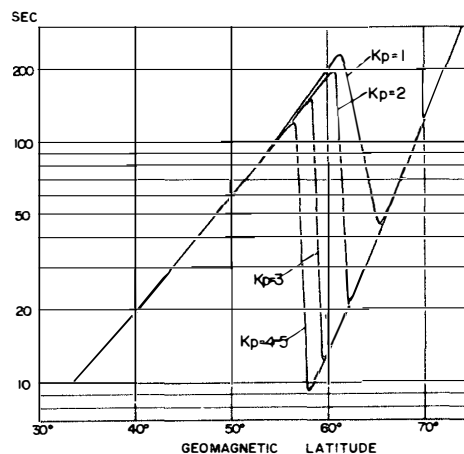


Fig. 47. Fundamental periods of the torsional oscillation of the lines of force in the nightside.

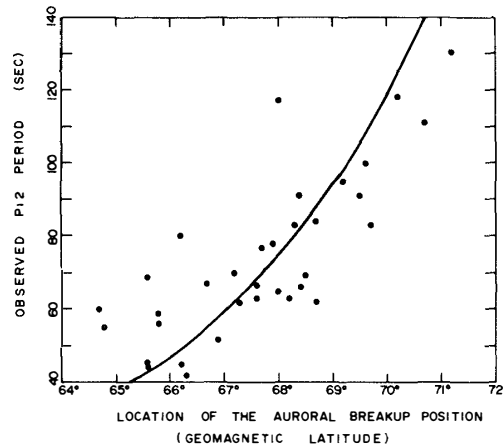


Fig. 48. Comparison between the observed Pi2 periods (solid circles) and the fundamental periods of the torsional oscillation of the lines of force in the auroral region (solid line).

ones and the results are illustrated in Fig. 48. The estimated periods agree with the observed Pi2 periods. The result seems to be related to the dipole-like magnetic field configuration in the nightside magnetosphere during the substorm expansion phase, as suggested by MCPHERRON *et al.* (1973) and PYTTE *et al.* (1976). MCPHERRON *et al.* (1973) found that the magnetic field observed at OGO 5 began to rotate from a tail-like orientation towards a dipole-like magnetic field configuration associated with the substorm expansion (Fig. 49). Recently, PYTTE *et al.* (1976) have investigated the dynamics of the magnetic tail in the local midnight region during the substorm, by referring to the data obtained by the multiple-satellites measurements (OGO 5 and Vela 4A). They showed that the magnetic field observed at OGO 5 which was reasonably assumed to be located near the field line reconnection region made clockwise rotations during the substorm expansions and became an almost dipolar field configuration near the maximum of the expansion phase. Similar tendency is also reported by WALKER *et al.* (1976), who studied the substorm associated boundary motion in the nightside magnetosphere on the basis of the data from ATS 6. They showed that in association with the substorm the boundary motions such as drawn in panel 3 in Fig. 50 are most frequently observed in the nightside. This fact is consistent with that the magnetic field configuration in the nightside magnetosphere varies from tail-like in the growth phase (KOKUBUN, 1977, 1978) to dipole like in the expansion phase.

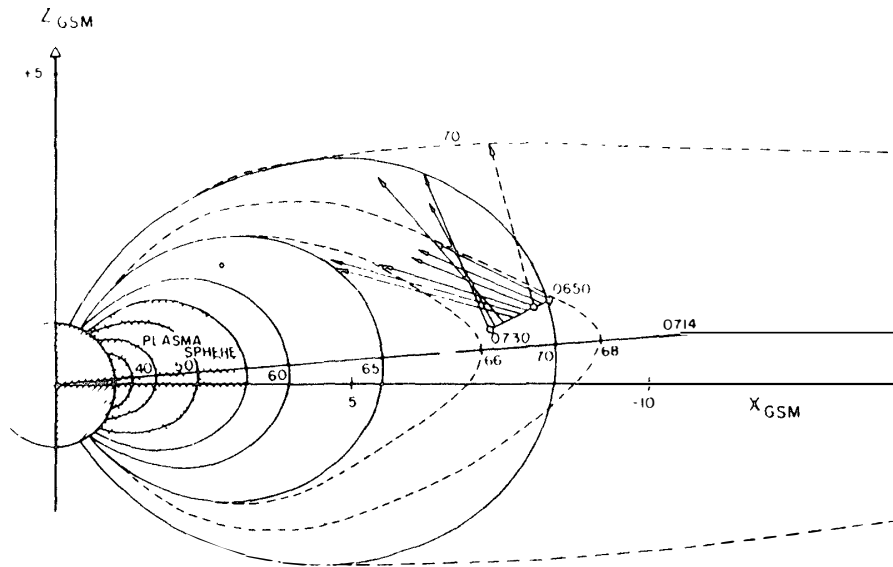


Fig. 49. Dipole-like magnetic field configuration during the substorm expansion, 0650-0730 UT on August 15, 1968 (After MCPHERRON *et al.*, 1973).

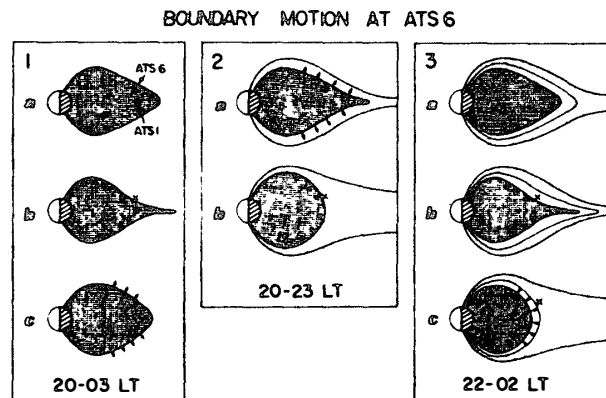


Fig. 50. Schematic diagram showing possible interpretation of boundary motion in the course of the magnetospheric substorm event (After WALKER *et al.*, 1976).

7.3. Latitudinal profile of Pi2 amplitudes

Several research workers have indicated that Pi2 amplitudes show a primary maximum under the auroral electrojet (SAITO, 1969; OLSON and ROSTOKER, 1975) and a secondary one near the plasmapause (RASPOPOV *et al.*,

1972; SAITO *et al.*, 1976). Similar relation is also found in the present work (Fig. 25).

A large gradient of the plasma density at the plasmopause causes a sharp change in the Alfvén velocity. Under such circumstances, an externally applied impulsive disturbance in association with the magnetospheric substorm can be coupled with an eigen oscillation of local resonant field lines around the plasmopause and a surface wave will be excited there (HASEGAWA and CHEN, 1974; SOUTHWOOD, 1974).

Using the data observed at a network of stations from $L=3.2$ to $L=4.4$ in the northern hemisphere and at their conjugate station in Antarctica, FUKUNISHI (1975) studied in detail the polarization changes of Pi2 pulsations associated with the plasmopause. He suggested that the Pi2 oscillations, which are originally excited at high latitudes in the magnetosphere, couple to the shear Alfvén waves of the resonant local field lines at the plasmopause. As is found in the results of Chapter 7.2 (Fig. 47), the fundamental period of the torsional oscillation of lines of force at the plasmopause are very similar to those in the auroral region.

The secondary Pi2 amplitude maximum shown in Fig. 25 is an evidence of the hydromagnetic wave resonance around the plasmopause in association with the substorm expansion.

7.4. Interpretation of Pi2 polarization features

In the previous section, it is suggested that Pi2 pulsations are standing oscillation of the lines of force anchored on the auroral oval. Such a model will be best examined by studying the Pi2 polarization features.

Many contradicting observational results have been reported on the polarization characteristics of the Pi2. On the basis of the data obtained at a low-latitude station, Onagawa in the northern hemisphere, KATO *et al.* (1956) indicated that the Pi2's are right-hand polarized in local pre-midnight hours and left-hand polarized in post-midnight hours. This relation is also seen in the results by SUTCLIFFE (1975a), who investigated the Pi2 polarization on the basis of the data obtained at a low-latitude station (Hermanus) in the southern hemisphere. On the other hand, CHRISTOFFEL and LINFORD (1966), ROSTOKER (1967), KOSHELEVSKIY *et al.* (1969), DOOVOV and MAINSTONE (1973) and SUTCLIFFE (1975a) showed that the polarization of the Pi2's observed in the region from the middle latitude to the sub-auroral zone (30° – 60° in geomagnetic latitude) is predominantly left-handed regardless of the occurrence local time. More recent important observations of the Pi2 polarization characteristics were given by BJÖRNSSON *et al.* (1971) and FUKUNISHI (1975). They showed that the sense of the Pi2 polarization reverses across the plasmopause from a left-hand polarization on the low-latitude side to a

right-hand polarization on the higher latitude side. SAKURAI(1970) showed statistically that the sense of polarization of the Pi2 event at College(64.7° in geomagnetic latitude) changes from a predominant left-hand polarization in the local pre-midnight hours to a predominant right-hand polarization in the local post-midnight hours, whereas the Pi2 at Point Barrow(68.5°) is predominantly right-hand polarized, regardless of the occurrence local time. According to OLSON and ROSTOKER(1975), the Pi2 observed at Fort Smith (67.3° in geomagnetic latitude) does not show any clear polarization characteristic.

At the present stage, it is very difficult to clarify the Pi2 polarization features over the wide area from auroral region to the low latitude. ROSTOKER (1967) tried to explain the presence of the occasional reversal of the Pi2 polarization by the ionospheric screening effect on the wave propagation. The Pi2 polarization features are studied in detail in the neighborhood of the auroral region, in the present work. The polarization reversals of the Pi2 are often observed across the auroral breakup region and the time of the Pi2 maximum occurrence as shown in Fig. 51a. The sense of the Pi2 polarization reverses across the auroral breakup region from a left-hand polarization on the lower-latitude side to a right-hand polarization on the higher latitude side before the time of maximum Pi2 occurrence(pre-midnight), whereas from a right-hand polarization on the lower-latitude side to a left-hand polarization on the higher-latitude side thereafter(post-midnight). Such polarization reversals were also found in the Pc5 events which were observed at high latitudes on the dayside(SAMSON *et al.*, 1971, 1972).

OBSERVED RESULT		
	PRE - MIDNIGHT	POST - MIDNIGHT
POLEWARD AE	R H	L H
EQUATORWARD AE	L H	R H

(a)

THEORETICAL ESTIMATION		
	$K_y < 0$	$K_y > 0$
$\frac{d}{dx}(\ln \frac{K_x}{K_y}) < 0$	R H	L H
$\frac{d}{dx}(\ln \frac{K_x}{K_y}) > 0$	L H	R H

(b)

Fig. 51. Relationship between the observed(a) and the theoretically evaluated(b) Pi2 polarization characteristics in the auroral region.

HASEGAWA and CHEN (1974), and SOUTHWOOD (1974) tried to interpret such polarization reversals theoretically. They indicated that the shear Alfvén (or anisotropic mode; $1 - K_z V_A / \omega^2 = 0$) and magnetosonic mode (or isotropic mode; $1 - K V_A / \omega^2 = 0$), must couple in the magnetosphere. In the above dispersion relation, K is the wave number, V_A is the Alfvén velocity and ω is the wave frequency. The characters of the polarization are determined from the following equation,

$$\frac{b_y}{b_x} = -iK_y \cdot \frac{V_A}{(\omega^2 - K_y V_A - K_z V_A)} \frac{d}{dx} (\ln \xi x)$$

where ξ and \mathbf{b} are the fluid displacement vector and the perturbed magnetic field vector. The ambient magnetic field $\mathbf{B} = B \cdot \mathbf{Z}$. The x direction is radially outward and the y direction is eastward, respectively. As the time dependence is expressed as $\exp(-i\omega t)$, the polarization with respect to the Z -direction is right-handed(left-handed) when the imaginary part of (b_y/b_x) is positive (negative). Hence, if the sense of the polarization is described for one looking down in the southern(northern) hemisphere, it is counter clockwise(clockwise) for the positive $K_y \cdot d(\ln \xi x)/dx$, whereas the opposite is the case for the negative $K_y \cdot d(\ln \xi x)/dx$. In the present case, a positive K_y corresponds to eastward propagation.

On the lower latitude side of the auroral breakup region where the Pi2 amplitude become maximum, the wave amplitude increases with increase of the radial distance [$d(\ln \xi x)/dx > 0$]. Therefore, if the Pi2 waves propagate westward ($K_y < 0$) before the time of maximum Pi2 occurrence, the polarization is estimated to be clockwise(left-handed) in the southern hemisphere. If the Pi2 waves propagate eastward ($K_y > 0$) after the time of maximum Pi2 occurrence, the sense of polarization is counter-clockwise(right-handed). On the higher latitude side of the auroral breakup region, the wave amplitude decreases with increase of the radial distance [$d(\ln \xi x)/dx < 0$] and the polarization is estimated to be counterclockwise(right-handed) before the time of maximum Pi2 occurrence and clockwise(left-handed) thereafter. These features are summarized in Fig. 51(b).

7.5. Generation mechanism of Pi2 pulsations

It is shown in the sections 7.1. and 7.2., that the Pi2 period is closely related to the location of the auroral breakup and its period behaviors can be explained by the fundamental torsional oscillations of the lines of force anchored on the midnight auroral oval. It is also shown in the section 7.3., that the Pi2 polarization characteristics in the auroral region can be interpreted by the odd mode standing oscillations.

Against the hydromagnetic waves theory, different generation mecha-

nisms were proposed by several research workers. It is well known that during magnetospheric substorms, several kinds of the magnetospheric and ionospheric current systems (e.g., westward auroral electrojet and Birkeland sheet currents) produce large magnetic effects on the ground. OLSON and ROSTOKER (1977) suggested that Pi2 pulsations in the auroral region is generated by sudden changes in the magnetospheric and ionospheric current systems proposed by ROSTOKER and BOSTROM (1976), which take place at the beginning of a substorm. WILHELM *et al.* (1977) tried to interpret the Pi2 as the magnetic effect of fluctuations of the auroral electrojet for the H-component, and the consequence of fluctuations of Birkeland sheet currents for the D-component.

If the magnetospheric and ionospheric current systems assumed by OLSON and ROSTOKER (1977) and WILHELM *et al.* (1977) play a fundamental role in the generation of Pi2 pulsations, the large (small) amplitude Pi2 would be observed in a case of the large (small) magnetic substorm which will be accompanied with intense (weak) ionospheric currents. In order to examine this prediction, relations between the Pi2 amplitude and the magnitude of the auroral current intensity are studied. Typical examples of very small and large substorm events are illustrated in Figs. 52a and b. In the event on September 1–2, 1973 (Fig. 52a), the onsets of the three small substorm were slightly identified by the small negative changes in the H-component concurrently observed at Mizuho and at Syowa at about 2250, 2330 UT

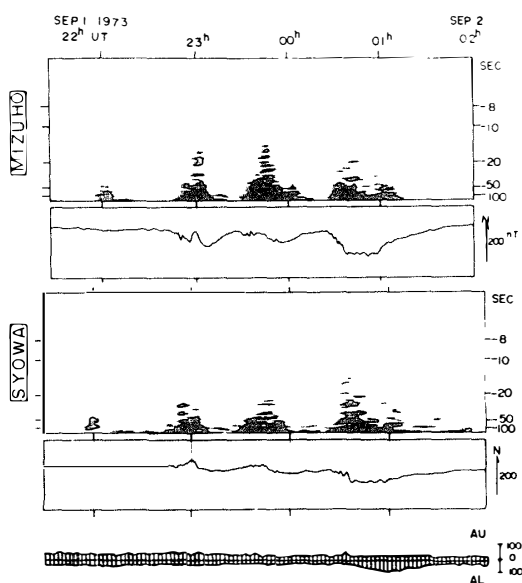


Fig. 52a. Dynamic spectra of ULF H-component, the simultaneous records of the geomagnetic H-component at Mizuho and Syowa and AU and AL indices (made at NOAA) on September 1, 1973.

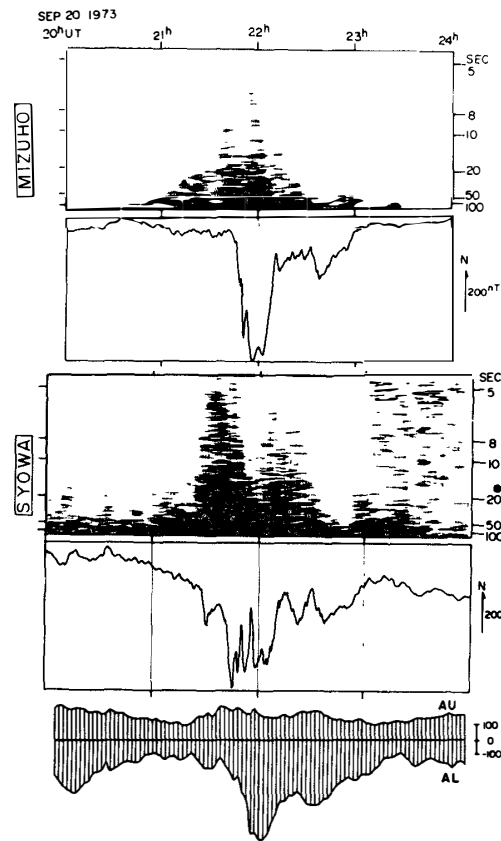


Fig. 52b. Dynamic spectra of ULF H-component, the simultaneous records of the geomagnetic H-component at Mizuho and Syowa, and AU and AL indices(made at NOAA) on September 20, 1973.

on September 1 and 0025 UT on September 2, respectively. AE index in the course of these three substorms did not have any clear indication of substorm activities as shown at the bottom in Fig. 52a. These facts suggest that the intensity of the ionospheric current system was weak or trivial in these events. In spite of those weak current intensities, the distinct Pi2's were observed simultaneously at Syowa and at Mizuho, as shown in the dynamic spectra. In association with these three small substorms, three distinct Pi2's were also observed at Hermanus(cf. Fig. 14b). The example of the large amplitude Pi2 occurrence over the wide latitude range during a small substorm has been already shown in Chapter 4 (Figs. 13a and b).

In a case of a large substorm event shown in Fig. 52b, the Pi pulsation observed at auroral stations in the beginning part of the large magnetic substorms consists of the Pi burst(irregular waveforms and localized) and Pi2(relatively regular waveforms and observed over the wide latitude range). In Fig. 52b, the localized large amplitude Pi bursts were intensified in associa-

tion with the sharp negative change of the H-component, around 2130 UT at Syowa and around 2150 UT at Mizuho. However, the Pi2 activities in this large event are not much larger comparing with those in the small one on September 1–2.

The relations among intensities of the auroral current system, auroral luminosity and Pi2's are examined on a statistical basis using magnitudes of the magnetic variation at Mizuho and Syowa, AE indices, intensities of auroral emission at Syowa and the Pi2 power intensities at Hermanus (low latitude station). The result is given in Fig. 53. It is obvious that there is little correlation among them. These results do not support the current system theory as a main cause of the Pi2.

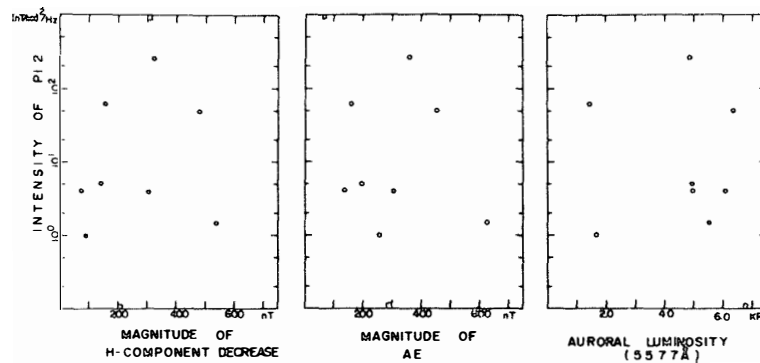


Fig. 53 Relationships among the Pi2 power intensity at Hermanus, magnitude of the H-component decrease in the auroral region, AE index and the intensity of the auroral luminosity.

Extensive studies have been made on changes of the magnetospheric field configuration associated with magnetospheric substorm (HONES *et al.*, 1970; NISHIDA and HONES, 1974; AKASOFU, 1977). It is generally believed that the substorm expansion is closely associated with the occurrence of magnetic field line reconnection in the magnetotail and the release of the stored energy of the magnetic field. Recently, it has been suggested that reconnection is initiated by the formation of a X type neutral line in the near-earth plasma sheet at the onset of the substorm (HONES *et al.*, 1970; NISHIDA and NAGAYAMA, 1973; NISHIDA and HONES, 1974). In a reconnection region in the magnetosphere, the magnetic field energy is transferred into particle energy ($E_p = B^2/8\pi$) causing a plasma instability there. Such plasma instability as well as a sudden formation of the dipole-like field lines from the tail-like ones may produce torsional Alfvén waves on the localized lines of force that cross the region of instabilities in the magnetosphere and the auroral oval on the ground, where the primary Pi2 amplitude maximum is

observed. Compressional waves can also exist in company with torsional ones (TAMAO, 1965; CHEN and HASEGAWA, 1974; SOUTHWOOD, 1974). These compressional waves will propagate in the magnetosphere inward to the earth and be transformed into surface waves at the boundary of the plasmapause, where an additional Pi2 amplitude maximum is observed. Those relations are schematically illustrated in Fig. 54. PYTTE *et al.* (1976) showed that the multiple expansions of the near-earth plasma sheet are intimately related to multiple onsets of Pi2 on the ground. In the present analyses, it is found that auroral breakup region of the multiple onset substorm shift systematically from low to high latitude and the associated Pi2 periods vary from short to long.

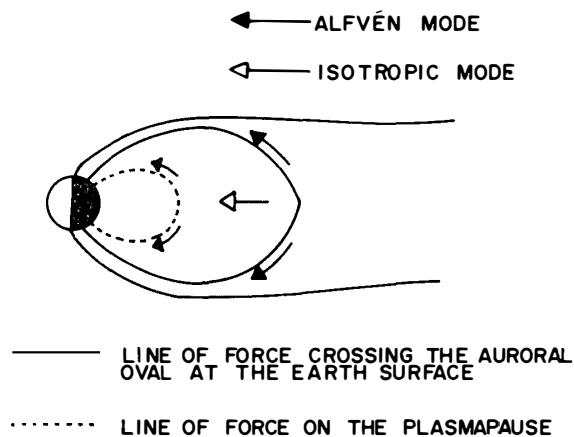


Fig. 54. Schematic diagrams showing the generation mechanism of the Pi2 pulsation.

7.6. Future work

As has been discussed, the Pi2 may be due to the hydromagnetic waves produced by the plasma instability. However, it is still unknown what kind of plasma instability is more effective. Recently, MALTSEV *et al.* (1974) proposed an Alfvén impulse originated in the ionosphere during a brightening of the aurora as a cause of the Pi2. According to their theoretical calculation, an electric impulse produced in the ionosphere by a sudden flare of the aurora will propagate along magnetic field lines with Alfvén velocity, and reflected from the ionosphere of the opposite hemisphere, it will form a standing Alfvén wave. Similar dynamical relation is also proposed by NISHIDA (1978). In addition to the above-mentioned mechanisms, a sudden formation of the dipole-like field lines from the tail like ones may produce torsional oscillations of the line of force as postulated by SAITO and SAKURAI (1970). These interesting problems will be examined as the next researching theme.

HUGHES and SOUTHWOOD(1974) showed that the relatively high conductivity of the ionosphere results in only a negligibly small vertical component of pulsations at the earth's surface. In addition, it is known(*e.g.* PRICE, 1968) that the induction in the earth's surface material produce anomalous vertical fields at pulsation period. Such ionospheric screening effect and earth induction effect are important problems to be discussed in future.

8. Concluding Remarks

In the present paper, the general characteristics and their interpretations of the magnetic Pi2 pulsations simultaneously observed in the auroral region, near the plasmopause and at the low latitudes were examined, and the following conclusions were reached.

(1) The Pi2 is simultaneously observed with the substorm expansion over the wide area from the auroral region to the low latitudes with approximately the similar predominant period. The Pi2 period is closely related to the location of auroral breakup, as it becomes shorter(longer) when the auroral breakup occurs at lower(higher) latitude.

(2) The Pi2 amplitude shows a primary maximum at the auroral oval and a secondary one at the plasmopause.

(3) The Pi2's with similar waveforms are simultaneously observed at the conjugate points in the auroral region in the wave-phase relations that the H-components oscillate almost in phase and the D-components oscillate almost out of phase.

(4) From the results of (1), (2) and (3), it is found that the Pi2 waves are generated by the odd mode standing oscillations of the resonant field lines localized at the auroral oval. This may be the fundamental mode, since the observed Pi2 period is very close to the fundamental period of the torsional oscillations of the lines of force anchored on the auroral oval in the local midnight.

(5) Concerning the Pi2 in the auroral region, the sense of its polarization reverses across the auroral oval from a left-hand polarization on the lower latitude side to a right-hand polarization on the higher latitude side before the time of the Pi2 maximum occurrence, and from a right-hand polarization on the lower latitude side to a left-hand polarization on the higher latitude side thereafter. Such polarization reversals result from the latitude dependence of the wave phase that the D-components oscillate in phase at the stations, whereas the oscillations in the H-components have large phase shifts across the auroral oval. If the Pi2 waves propagate westward before the time

of Pi2 maximum occurrence(pre-midnight) and eastward thereafter(post-midnight), those observed polarization characteristics can be interpreted by the coupling resonance oscillations between the hydromagnetic shear Alfvén and magnetosonic waves as calculated by CHEN and HASEGAWA(1974) and SOUTHWOOD(1974).

(6) There is little correlation between the Pi2 power intensity and the intensity of the auroral electrojet or the auroral particle precipitation. It is difficult to consider the current system in the magnetosphere and ionosphere (OLSON and ROSTOKER,1977; WILHELM,1977) as a main cause of the Pi2.

(7) The most plausible generation mechanism of the Pi2 is the torsional hydromagnetic oscillations of the localized lines of force that cross the region of the plasma instability in the magnetosphere and the auroral oval on the ground. Compressional waves which also exist in company with torsional Alfvén ones will propagate in the magnetosphere inward to the earth and will be transformed into surface waves at the plasmopause, where an additional secondary Pi2 amplitude maximum is observed.

Acknowledgments

The author wishes to express his thank to all members of the 14th wintering party of the Japanese Antarctic Research Expedition for their kind support in making the observations at Syowa and Mizuho Stations, Antarctica. Special thanks are due to Professor T. HIRASAWA of the National Institute of Polar Research, the reader of the 14th wintering party of the Japanese Antarctic Research Expedition. The author greatly indebted to the hospitality and encouragement of Professor T. SAITO of the Tohoku University, Dr. K. YANAGIHARA, the former director of the Kakioka Magnetic Observatory and Dr. M. KAWAMURA, the director of the Kakioka Magnetic Observatory. The author is also grateful to Drs. R. G. CURRIE and P. R. SUTCLIFFE of the Hermanus Magnetic Observatory, South Africa, and Professor T. WATANABE of the University of British Columbia, Canada, for suggestions on the application of the analysis methods. His thank is due to Professors S. KOKUBUN of the Tokyo University and H. FUKUNISHI of the National Institute of Polar Research for their valuable critiques on manuscript.

The author is especially grateful to the following people for sending the geomagnetic data at his request.

a) Dr. M. D. BARKER of the Department of Physics, University of Natal of South Africa for the data at Sanae.

b) The Director of Hermanus Magnetic Observatory, South Africa for the data at Hermanus.

c) The Director of Antarctic Geomagnetic and Aurora Programme, South Africa for the data at Sanae.

d) The Director of Bureau of Mineral Resources, Geology and Geophysics, Australia for the data at Mawson.

e) The Director of Antarctic Division, Australia for the data at Mawson.

f) The Director of Geophysical Department, Arctic and Antarctic Research Institute of USSR for the data at Novolazarevskaya and Molodezhnaya.

g) The Director of the Reykjavik Magnetic Observatory Iceland for the data of Reykjavik.

h) The Director of World Data Center A for Solar-Terrestrial Physics, Environmental Data Service, NOAA for the data of AU, AL, AO and AE indices.

References

- AKASOFU, S.-I. (1965): Dynamical morphology of auroras. *Space Sci. Rev.*, **4**, 498–540.
- AKASOFU, S.-I. (1968): *Polar and Magnetospheric Substorms*. Dordrecht, D. Reidel, 280p.
- AKASOFU, S.-I. (1977). *Physics of Magnetospheric Substorms*. Dordrecht, D. Reidel, 599p.
- AKASOFU, S.-I. and CHAPMAN, S. (1963): The lower limit of latitude (US sector) of northern quiet auroral arcs, and its relation to Dst (H). *J. Atmos. Terr. Phys.*, **25**, 9–12.
- ANGENHEISTER, G. (1912): Über die Fortpflanzungsgeschwindigkeit magnetischer Störungen und Pulsationen. Bericht über die erdmagnetischen Schnellregistrierungen in Apia (Samoa), Batavia, Cheltenham, und Tsingtau in September 1911, in *Göttingen Nach. Ges. Wiss.*, 568p.
- BINSACK, N.J. (1967): Plasmopause observations with the M.I.T. experiment on Imp. 2. *J. Geophys. Res.*, **72**, 5231–5238.
- BJÖRNSSON, A., HILLEBRAND, O. and VOELKER, H. (1971): First observational results of geomagnetic Pi2 and Pc5 pulsations on a north-south profile through Europe. *Z. Geophys.*, **37**, 1031–1050.
- BLACKMAN, R.B. and TUKEY, S.W. (1958). *The Measurement of Power Spectra*. New York, Dover, 190p.
- BURG, J.P. (1967): Maximum entropy spectral analysis. Paper presented at the 37th Annual International Meeting, Soc. of Explor. Geophys., Oklahoma City, Okla., Oct. 31.
- BURG, J.P. (1972): The relationship between maximum entropy spectra and maximum likelihood spectra. *Geophysics*, **37**, 375–376.
- CARPENTER, D.L. and STONE, K. (1967): Direct detection by a whistler method of the magnetospheric electric field associated with a polar substorm. *Planet. Space Sci.*, **15**, 395–397.
- CHANNON M.J. and ORR, D. (1970): A study of equatorial geomagnetic micropulsations. *Planet. Space Sci.*, **18**, 229–237.
- CHAPPELL, C.R. (1972): Recent satellite measurements of the morphology and dynamics of the plasmasphere. *Rev. Geophys. Space Phys.*, **10**, 951–979.
- CHAPPELL, C.R., HARRIS, K.K. and SHARP, G.W. (1970): A study of the influence of magnetic activity on the location of the plasmopause as measured by Ogo 5. *J. Geophys. Res.*, **75**, 50–56.
- CHRISTOFFEL, D.A. and LINFORD, J.G. (1966): Diurnal properties of the horizontal geomagnetic micropulsation field in New Zealand. *J. Geophys. Res.*, **71**, 891–897.
- COOLEY, J.W. and TUKEY, T.W. (1965): An algorithm for machine calculation of complex Fourier series. *Math. Comp.*, **19**, 297–301.
- CUMMINGS, W.D., O'SULLIVAN, R.J. and COLEMAN, P.J., Jr. (1969): Standing Alfvén waves in the magnetosphere. *J. Geophys. Res.*, **74**, 778–793.
- CURRIE, R.G. (1974): Harmonics of the geomagnetic annual variation. *J. Geomagn. Geoelectr.*, **26**, 319–328.
- DOBOV, A.L. (1973): Frequency and period relationships for Pi2 micropulsations. *Planet. Space Sci.*, **21**, 532–534.
- DOBOV, A.L. and MAINSTONE, J.S. (1973): Investigations of Pi2 micropulsations - (I) Frequency spectra and polarization. *Planet. Space Sci.*, **21**, 721–730.
- DOBOV, A.L. and MAINSTONE, J.S. (1973). Investigations of Pi2 micropulsations - (II) Relevance of observations to generation theories. *Planet. Space Sci.*, **21**, 731–740.
- DUNGEY, J.W. (1954): *Electrodynamics of the outer atmosphere*. The Pennsylvania State Univ., Sci. Rep., **69**, 229–236.
- FELDSTEIN, Y. I. and STARKOV, G.V. (1968): Auroral oval in the IGY and IQSY period and a ring current in the magnetosphere. *Planet. Space Sci.*, **16**, 129–133.

- FUKUNISHI, H.(1973):Mizuho Kansokukyoten ni okeru chijiki myakudô kansoku hôkoku (Observations of geomagnetic pulsations in the winter of 1970 at Mizuho Camp). Nankyoku Shiryo (Antarct. Rec.), 47, 39–45.
- FUKUNISHI, H. (1975): Polarization changes of geomagnetic Pi2 pulsations associated with the plasmopause. J. Geophys. Res., 80, 98–110.
- FUKUNISHI, H. and HIRASAWA, T. (1970): Progressive changes in Pi2 power spectra with the development of magnetospheric substorm. Rep. Ionos. Space Res. Jpn., 24, 45–65.
- FUKUNISHI, H. and TOHMATSU, T. (1973). Constitution of proton aurora and electron aurora substorms, Part I. Meridian scanning photometer system for proton and electron auroras. JARE Sci. Rep., Ser. A (Aeronomy), 11, 1–18.
- HASEGAWA, A. and CHEN, L. (1974): Theory of magnetic pulsations. Space Sci. Rev., 16, 347–359.
- HEACOCK, R.R. and HESSLER, V.P. (1963): Telluric current micropulsation bursts. J. Geophys. Res., 68, 953–954.
- HIRASAWA, T. and NAGATA, T. (1966): Spectral analysis of geomagnetic pulsations from 0.5 to 100 sec in period for the quiet sun condition. Pure Appl. Geophys., 65, 102–124.
- HIRASAWA, T. and NAGATA, T. (1972): Constitution of polar substorm and associated phenomena in the southern polar region. JARE Sci. Rep., Ser. A (Aeronomy), 10, 76p.
- HONES, E.W., Jr., AKASOFU, S.-I., PERREAULT, P., BAME, S.J. and SINGER, S. (1970): Poleward expansion of the auroral oval and associated phenomena in the magnetotail during auroral substorms, 1. J. Geophys. Res., 75, 7060–7074.
- HUGHES, W.J. and SOUTHWOOD, D.J. (1974): Effect of atmosphere and ionosphere on magnetospheric micropulsation signals. Nature, 248, 493–495.
- INOUE, Y. (1973). Wave polarizations of geomagnetic pulsations observed in high latitudes on the earth's surface. J. Geophys. Res., 78, 2959–2976.
- JACOBS, J.A. (1968): Pi events with particular reference to conjugate point phenomena. Radio Sci., 3, 539–544.
- JACOBS, J.A. (1970): Geomagnetic Micropulsations. Physics and Chemistry in Space, Vol. 1, ed. by J.G. ROEDERER. Berlin, Springer, 215p.
- KAN, J.R. and AKASOFU, S.-I. (1976): Energy source and mechanism for accelerating the electrons and driving the field-aligned currents of the discrete auroral arc. J. Geophys. Res., 81, 5123–5130.
- KANASEWICH, E.R. (1975): Time Sequence Analysis in Geophysics. Edmonton, The University of Alberta Press, 364p.
- KATO, Y. (1977): Investigation of the geomagnetic pulsation. Tokyo, Tokai University Press, 69p.
- KATO, Y., SAITO, T. and KONDO, M. (1961): Geomagnetic rapid variations observed at Onagawa Magnetic Observatory during the International Geophysical Year, Part 2. Sci. Rep. Tohoku Univ., Ser. 5: Geophys., 12, 1–75.
- KATO, Y., OSSAKA, J., OKUDA, M., WATANABE, T. and TAMAO, T. (1956): Investigation on the magnetic disturbance by the induction magnetograph, Part V, On the rapid pulsation, P.S.C.. Sci. Rep. Tohoku Univ., Ser. 5: Geophys., 7, 136–146.
- KAWAMURA, M. (1970): Short-period geomagnetic micropulsations with low latitudes. Geophys. Mag., 35, 1–54.
- KISABETH, J.L. and ROSTOKER, G. (1974): The expansive phase of magnetospheric substorms 1. Development of the auroral electrojets and auroral arc configuration during a substorm. J. Geophys. Res., 79, 972–984.
- KOKUBUN, S. (1977): Problems of the auroral substorms. Proceeding of the IMS Symposium, 197–202.
- KOKUBUN, S. (1978): Substorm signature at synchronous orbit. The 63rd Annual Meeting of Japanese Society of Geomagnetism and Geoelectricity, 27.

- KOSHELEVSKIY, V.K., BARANSKIY, L.N., RASPOPOV, O.M., TROITSKAYA, V.A. and SCHLICH, R. (1968): Spectral characteristics of type Pi2 geomagnetic field pulsations. *Geomagn. Aeron.*, **8**, 416–420.
- KUWASHIMA, M. (1974a): Concurrent geomagnetic observations at Syowa and Mizuho Stations in Antarctica, 1. The 55th Annual Meeting of Japanese Society of Geomagnetism and Geoelectricity, 44.
- KUWASHIMA, M. (1974b): Concurrent geomagnetic observations at Syowa and Mizuho Stations, in Antarctica, 2. The 56th Annual Meeting Japanese Society of Geomagnetism and Geoelectricity, 30.
- KUWASHIMA, M. (1975): Some characters of substorm-associated geomagnetic phenomena in the southern polar region (I). *Mem. Kakioka Magn. Obs.*, **16**, 95–110.
- LANZEROTTI, L.J. (1974): Magnetic pulsation conjugacy and its mechanisms. *Mem. Natl Inst. Polar Res., Spec. Issue*, **3**, 61–76.
- LANZEROTTI, L.J. and FUKUNISHI, H. (1974): Modes of magnetohydrodynamic waves in the magnetosphere. *Rev. Geophys. Space Phys.*, **12**, 724–729.
- LANZEROTTI, L.J. and FUKUNISHI, H. (1975): Relationships of the characteristics of magnetohydrodynamic waves to plasma density gradients in the vicinity of the plasmopause. *J. Geophys. Res.*, **80**, 4627–4634.
- LANZEROTTI, L.J., FUKUNISHI, H. and MACLENNAN, C.G. (1976): Observations of magnetohydrodynamic waves on the ground and on a satellite. *J. Geophys. Res.*, **81**, 4537–4545.
- MALTSEV, YU.P., LEONTYEV, S.V. and LYATSKY, W.B. (1974): Pi2 pulsations as a result of evolution of an Alfvén impulse originating in the ionosphere during a brightening of aurora. *Planet. Space Sci.*, **22**, 1519–1533.
- MCDONOUGH, R.N. (1974): Maximum-entropy spatial processing of array data. *Geophysics*, **39**, 843–851.
- MCPHERRON, R.L., AUBRY, M.P., RUSSEL, C.T., and COLEMAN, P.J., Jr. (1973): Satellite studies of magnetospheric substorms on August 15, 1968, 4. Ogo 5 magnetic field observations. *J. Geophys. Res.*, **78**, 3068–3078.
- NAGATA, T., HIRASAWA, T., AYUKAWA, M. and FUKUNISHI, H. (1976): Multipoint ground observations around Syowa Station, Antarctica by means of unmanned and automatic observatories. *Mem. Natl Inst. Polar Res., Spec. Issue*, **6**, 44–51.
- NISHIDA, A. (1978): Oscillations of tail-ionosphere coupling current. The 63rd Annual Meeting of Japanese Society of Geomagnetism and Geoelectricity, 17.
- NISHIDA, A. and NAGAYAMA, N. (1973): Synoptic survey for the neutral line in the magnetotail during the substorm expansion phase. *J. Geophys. Res.*, **78**, 3782–3798.
- NISHIDA, A. and HONES, E.W., Jr. (1974): Association of plasma sheet thinning with neutral line formation in the magnetotail. *J. Geophys. Res.*, **79**, 535–547.
- OBAYASHI, T. and JACOBS, J.A. (1958): Geomagnetic pulsation and the earth's outer atmosphere. *Geophys. J. R. Astron. Soc.*, **1**, 53–63.
- OLSON, J.V. and ROSTOKER, G. (1975): Pi2 pulsations and the auroral electrojet. *Planet. Space Sci.*, **23**, 1129–1139.
- OLSON, J.V. and ROSTOKER, G. (1977): Latitude variation of the spectral components of an auroral zone Pi2. *Planet. Space Sci.*, **25**, 663–671.
- ORR, D. (1973): Magnetic pulsations within the magnetosphere: A review. *J. Atmos. Terr. Phys.*, **35**, 1–50.
- ORR, D. and MATTHEV, A.D. (1971): The variation of geomagnetic micropulsation periods with latitude and the plasmopause. *Planet. Space Sci.*, **19**, 897–905.
- PERKINS, D.M., WATANABE, T. and WARD, S.H. (1972): Relations between geomagnetic micropulsations and magnetotail field changes. *J. Geophys. Res.*, **77**, 159–171.
- PRICE, A.T. (1968): Effects of induced earth currents on low-frequency electromagnetic oscillations. *Radio Sci.*, **69D**, 1161–1168.

- PYTTE, T., MCPHERRON, R.L. and KIVELSON, M.G. (1976): Multiple-satellite studies of magnetospheric substorms; Radial dynamics of the plasma sheet. *J. Geophys. Res.*, **81**, 5921–5933.
- RANKIN, D. and KURTZ, R. (1970): Statistical study of micropulsation polarizations. *J. Geophys. Res.*, **75**, 5444–5458.
- RASPOPOV, O.M., TROITSKAYA, V.A., BARANSKIY, L.N., BELEN'KAYA, B.N., KOSHELEVSKIY, V.K., AFANS'YEVA, L.T., ROX, J. and FAMBITOKOYA, N.L. (1972): Properties of geomagnetic Pi2 pulsation spectra along a meridional profile. *Geomagn. Aeron.*, **12**, 772–775.
- ROSTOKER, G. (1965): Propagation of Pi2 micropulsations through the ionosphere. *J. Geophys. Res.*, **70**, 4388–4390.
- ROSTOKER, G. (1967): The frequency spectrum of Pi2 micropulsation activity and its relationship to planetary magnetic activity. *J. Geophys. Res.*, **72**, 2032–2039.
- ROSTOKER, G. and BOSTRÖM, R. (1976): A mechanism for driving the gross Birkeland current configuration in the auroral oval. *J. Geophys. Res.*, **81**, 235–244.
- RYCROFT, M.J. and THOMAS, J.O. (1970): The magnetospheric plasmopause and the electron density trough at the Alouette I orbit. *Planet. Space Sci.*, **18**, 65–80.
- SAITO, T. (1960): Period analysis of geomagnetic pulsations by a sona-graph method. *Sci. Rep. Tohoku Univ.*, Ser. 5: *Geophys.*, **12**, 105–113.
- SAITO, T. (1961): Oscillation of geomagnetic field with the progress of pt-type pulsation. *Sci. Rep. Tohoku Univ.*, Ser. 5: *Geophys.*, **13**, 53–61.
- SAITO, T. (1964): Mechanism of geomagnetic continuous pulsations and Physical states of the exosphere. *J. Geomagn. Geoelectr.*, **16**, 115–151.
- SAITO, T. (1967): Some characteristics of the dynamic spectrum of long-period dynamic spectrum geomagnetic pulsations. *J. Geophys. Res.*, **72**, 3895–3904.
- SAITO, T. (1969): Geomagnetic pulsations. *Space Sci. Rev.*, **10**, 319–412.
- SAITO, T. (1972): Some topics for the study of the mechanism of magnetospheric substorm by means of rocket observation in the auroral zone. *Nankyoku Shiryo (Antarct. Rec.)*, **43**, 65–79.
- SAITO, T. (1974a): Examination of the models for the substorm-associated magnetic pulsation, Ps 6. *Sci. Rep. Tohoku Univ.*, Ser. 5: *Geophys.*, **22**, 35–59.
- SAITO, T. (1974b): Study of magnetospheric substorm by means of a magnetic pulsation Pi2. *Proc. Substorm Workshop, Sendai*, 87–94.
- SAITO, T. and MATSUSHITA, S. (1967): Geomagnetic pulsations associated with sudden commencements and sudden impulses. *Planet. Space Sci.*, **15**, 573–587.
- SAITO, T. and MATSUSHITA, S. (1968): Solar cycle effects on geomagnetic Pi2 pulsations. *J. Geophys. Res.*, **73**, 267–286.
- SAITO, T. and SAKURAI, T. (1970): Mechanism of geomagnetic Pi2 pulsations in magnetically quiet condition. *Sci. Rep. Tohoku Univ.*, Ser. 5: *Geophys.*, **20**, 49–70.
- SAITO, T., SAKURAI, T. and KOYAMA, Y. (1976a): Mechanism of association between Pi2 pulsation and magnetospheric substorm. *J. Atmos. Terr. Phys.*, **38**, 1265–1277.
- SAITO, T., YUMOTO, K. and KOYAMA, Y. (1976b): Magnetic pulsation Pi2 as a sensitive indicator of magnetospheric substorm. *Planet. Space Sci.*, **24**, 1025–1029.
- SAKURAI, T. (1970): Polarization characteristics of geomagnetic Pi2 micropulsations. *Sci. Rep. Tohoku Univ.*, Ser. 5: *Geophys.*, **20**, 107–117.
- SAKURAI, T. and SAITO, T. (1976a): Magnetic pulsation Pi2 and substorm onset. *Planet. Space Sci.*, **24**, 573–575.
- SAKURAI, T. and SAITO, T. (1976b): Effect of the substorm phases on the electric field variation near the plasmopause inferred by the pulsation-pearl method. *J. Atmos. Terr. Phys.*, **38**, 1169–1175.
- SAMSON, J.C., and ROSTOKER, G. (1972): Latitude-dependent characteristics of high-latitude Pc4 and Pc5 micropulsations. *J. Geophys. Res.*, **77**, 6133–6144.
- SAMSON, J.C., JACOBS, J.A. and ROSTOKER, G. (1971): Latitude-dependent characteristics of long-period geomagnetic micropulsations. *J. Geophys. Res.*, **76**, 3675–3683.

- SMITH, B.P. (1973): On the occurrence of Pi2 micropulsations. *Planet. Space Sci.*, **21**, 831–837.
- SMYLIE, D.E., CLARKE, G.K.C. and ULRYCH, T.J. (1973): Analysis of irregularities in the earth's rotation. *Methods in Computational Physics*, Vol. 13, ed. by B. ALDER. New York, Academic Press, 391–430.
- SOUTHWOOD, D.J. (1974a): Recent studies in micropulsation theory. *Space Sci. Rev.*, **16**, 413–425.
- SOUTHWOOD, D.J. (1974b): Some features of field line resonances in the magnetosphere. *Planet. Space Sci.*, **22**, 483–491.
- STRINGER, W.J. and BELON, A.E. (1967): The statistical auroral zone during IQSY, and its relationship to magnetic activity. *J. Geophys. Res.*, **72**, 245–250.
- STRINGER, W.J., BELON, A.E. and AKASOFU, S.-I. (1965): The latitude of auroral activity during periods of zero and very weak magnetic disturbance. *J. Atmos. Terr. Phys.*, **27**, 1039–1044.
- STUART, W.F. (1972): Associations between Pi2 and Bays at Lerwick and Halley Bay. *J. Atmos. Terr. Phys.*, **34**, 817–827.
- STUART, W.F. (1972): A special feature of impulsive pulsations (Pi2). *J. Atmos. Terr. Phys.*, **34**, 829–836.
- STUART, W.F. (1976): Features of the generation of dPi's derived from conjugate observations. *J. Atmos. Terr. Phys.*, **38**, 271–278.
- STUART, W.F. and BOOTH, D.C. (1974): A study of the power spectra of dPi's and Pi2's. *J. Atmos. Terr. Phys.*, **36**, 835–849.
- SUGIURA, M. and WILSON, C.R. (1964): Oscillation of the geomagnetic field lines and associated magnetic perturbations at conjugate points. *J. Geophys. Res.*, **69**, 1211–1216.
- SUTCLIFFE, P.R. (1974): Improved resolution in Pi2 magnetic pulsation power spectra. *Planet. Space Sci.*, **22**, 1461–1470.
- SUTCLIFFE, P.R. (1975a): The power spectra of irregular magnetic pulsations. Doctoral thesis, Potchefstroom Univ., 95p.
- SUTCLIFFE, P.R. (1975b): The association of harmonics in Pi2 power spectra with the plasmapause. *Planet. Space Sci.*, **23**, 1581–1587.
- TAMAO, T. (1965). Transmission and coupling resonance of hydromagnetic disturbances in the non-uniform earth's magnetosphere. *Sci. Rep. Tohoku Univ.*, Ser. 5: *Geophys.*, **17**, 43–72.
- TROITSKAYA, V.A. (1967): Micropulsations and the state of the magnetosphere. *The Solar-Terrestrial Physics*, ed. by J.W. King and W.S. NEWMAN. New York, Academic Press, 213–274.
- ULRYCH, T.J. and BISHOP, T.N. (1975): Maximum entropy spectral analysis and autoregressive decomposition. *Rev. Geophys.*, **13**, 183–200.
- WALKER, R.J., ERICKSON, K.N., SWANSON, R.L. and WINCKLER, J.R. (1976): Substorm-associated particle boundary motion at synchronous orbit. *J. Geophys. Res.*, **81**, 5541–5550.
- WATANABE, T. (1959): Hydromagnetic oscillations of the outer ionosphere and geomagnetic pulsation. *J. Geomagn. Geoelectr.*, **10**, 195–202.
- WATANABE, T. (1961): On the origins of geomagnetic pulsations. *Sci. Rep. Tohoku Univ.*, Ser. 5: *Geophys.*, **13**, 127–140.
- WESTPHAL, K.O. and JACOBS, J.A. (1962): Oscillations of earth's outer atmosphere and micropulsations. *J. R. Astron. Soc. Canada*, **6**, 360–376.
- WILHELM, K., MÜNCH, J.W. and KREMSER, G. (1977): Fluctuations of the auroral zone current system and geomagnetic pulsations. *J. Geophys. Res.*, **82**, 2705–2716.
- YANAGIHARA, K. (1960): Geomagnetic pulsations in middle latitudes—morphology and its interpretation. *Mem. Kakioka Magn. Obs.*, **9**, 15–74.

- YANAGIHARA, K. (1963): Geomagnetic micropulsations with periods from 0.03 to 10 seconds in the auroral zone with special reference to conjugate-point studies. *J. Geophys. Res.*, **68**, 3383–3397.

*(Manuscript received October 20, 1977;
Revised manuscript received August 30, 1978)*